

# Amino Acid Homeostasis Modulates Salicylic Acid–Associated Redox Status and Defense Responses in *Arabidopsis*

Guosheng Liu,<sup>a</sup> Yuanyuan Ji,<sup>a</sup> Nazmul H. Bhuiyan,<sup>a</sup> Guillaume Pilot,<sup>b</sup> Gopalan Selvaraj,<sup>c</sup> Jitao Zou,<sup>c</sup> and Yangdou Wei<sup>a,1</sup>

<sup>a</sup> Department of Biology, University of Saskatchewan, Saskatoon, Saskatchewan S7N 5E2, Canada

<sup>b</sup> Department of Plant Biology, Carnegie Institution for Science, Stanford, California 94305

<sup>c</sup> Plant Biotechnology Institute, National Research Council of Canada, Saskatoon, Saskatchewan S7N 0W9, Canada

**The tight association between nitrogen status and pathogenesis has been broadly documented in plant–pathogen interactions. However, the interface between primary metabolism and disease responses remains largely unclear. Here, we show that knockout of a single amino acid transporter, LYSINE HISTIDINE TRANSPORTER1 (LHT1), is sufficient for *Arabidopsis thaliana* plants to confer a broad spectrum of disease resistance in a salicylic acid–dependent manner. We found that redox fine-tuning in photosynthetic cells was causally linked to the *lht1* mutant-associated phenotypes. Furthermore, the enhanced resistance in *lht1* could be attributed to a specific deficiency of its main physiological substrate, Gln, and not to a general nitrogen deficiency. Thus, by enabling nitrogen metabolism to moderate the cellular redox status, a plant primary metabolite, Gln, plays a crucial role in plant disease resistance.**

## INTRODUCTION

The successful invasion of various plant pathogens depends both on their ability to evade the defense mechanisms of the host and to use the available nutrient sources offered by the host. Thus, pathogens have evolved distinct lifestyles, including biotrophy, hemibiotrophy, and necrotrophy, that allow them to succeed (Solomon et al., 2003; Divon and Fluhr, 2007). However, the molecular mechanisms underlying the central metabolic aspects of plant–pathogen interactions are poorly understood. Nitrogen (N) metabolism is a case in point now that available data for the role of N in disease appear rudimentary and even contradictory in most cases (Solomon et al., 2003; Walters and Bingham, 2007). The competition for a N source between the pathogen and its host is a dynamic and complex process. Not only are pathogen infection and colonization affected by the N status but so are host N metabolism and translocation per se altered or manipulated during pathogen attack (Divon and Fluhr, 2007; Snoeijers et al., 2000). Therefore, understanding how plants trade off the essential nutrients for balancing basal defense with growth and development has recently attracted much attention (Berger et al., 2007; Spoel et al., 2007).


Plants contain N in the form of nitrate, ammonia, amino acids, amides, nucleic acids, and proteins. Organic Gln is the metabolic entry point and primary assimilation product for inorganic N ( $\text{NO}_3^-$

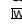
and  $\text{NH}_4^+$ ), which is subsequently metabolized to the other three major amino acids, Glu, Asp, and Asn, and eventually to all other amino acids (Coruzzi, 2003). Glutamine synthetase (GS), coupled with glutamate synthase (GOGAT), is the key enzyme catalyzing the primary and secondary assimilation of  $\text{NH}_4^+$ . In most plants, GS has two spatially distinct isoforms: cytosolic GS1 and plastidic GS2, the latter of which is critical for primary N assimilation (Coruzzi, 2003). In plants, GS activity is regulated at the protein level, and oxidative modification of GS has been implicated as the first step in the turnover of GS (Ortega et al., 1999; Palatnik et al., 1999). Susceptibility of GS to reactive oxygen/nitrogen species has also been found in cyanobacterium (Gómez-Baena et al., 2006), which suggests that GS might be a target of oxidative stresses (Motohashi et al., 2001). Growing evidence indicates that the expression of GS2 is suppressed in plant leaf tissues during pathogen attack, whereas that of GS1 is induced (Pageau et al., 2006; Perez-Garcia et al., 1995, 1998), suggesting an intricate spatiotemporal regulation of Gln biosynthesis in the host during pathogen infection. Indeed, there is evidence for amino acid homeostasis playing a role in plant defense, as revealed in studies on aminotransferases or homoserine kinase (Song et al., 2004; Taler et al., 2004; van Damme et al., 2009).

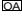
In addition to de novo biosynthesis, the uptake and translocation of amino acids also impact the N status and concentration in plant tissues. Plants have a multitude of amino acid transporters, which display different substrate selectivity and subcellular distribution and likely function in intra- and intercellular transport, the capture of amino acids from the apoplast, and uptake of amino acids from the soil (Fischer et al., 1998). The *Arabidopsis thaliana* genome contains five gene families comprising at least 67 genes whose products have been annotated as putative amino acid transporters (Rentsch et al., 2007). How these transporters impact N homeostasis during pathogenesis remains unknown.

<sup>1</sup> Address correspondence to yangdou.wei@usask.ca.

The author responsible for distribution of materials integral to the findings presented in this article in accordance with the policy described in the Instructions for Authors (www.plantcell.org) is: Yangdou Wei (yangdou.wei@usask.ca).

 Some figures in this article are displayed in color online but in black and white in the print edition.

 Online version contains Web-only data.

 Open Access articles can be viewed online without a subscription. www.plantcell.org/cgi/doi/10.1105/tpc.110.079392

Plants have complex immune mechanisms against pathogens (Jones and Dangl, 2006), the basal defense response being one of them. It operates in both incompatible and compatible interactions and is effective after recognition of the pathogen by host surveillance systems. Both positive and negative regulators have been identified in defense system, and, among these, most is known about the positive regulator, phenolic compound salicylic acid (SA). SA is synthesized in chloroplasts via the Phe pathway and/or the chorismate (the precursor of Phe) pathway (Wildermuth et al., 2001). SA accumulation has been widely used as a reliable marker of elevated defense responses and is closely associated with redox homeostasis, hypersensitive cell death, or systemic acquired resistance (Dong, 2004; Song et al., 2004); however, the exact role of SA in defense networks remains elusive. To identify novel components of the SA-associated defense pathway and to extend our work on the role of iron homeostasis in plant defense responses (Liu et al., 2007b), we investigated the roles of various *Arabidopsis* transporters, including amino acid/polyamine transporters/permeases, in disease resistance. We revealed that an amino acid transporter, LYSINE HISTIDINE TRANSPORTER1 (LHT1) (Chen and Bush, 1997; Hirner et al., 2006), is involved in the development of disease symptoms. Further investigations demonstrated that LHT1 is a negative modulator of disease resistance and that its substrate, Gln, when integrated with the SA pathway, plays pivotal roles in plant defense responses. Our results provide insight into how a primary metabolite (i.e., Gln) influences the plant defense response.

## RESULTS

### Disruption of *LHT1* Enhances Disease Resistance to a Broad Spectrum of Pathogens

In our survey of mutations in amino acid/polyamine transporter/permease-like genes in *Arabidopsis* that alter their response to pathogen infection and SA treatment, we found that a T-DNA insertion mutation in the At5g40780 locus resulted in strong leaf chlorosis. At5g40780 was initially designated as a basic amino acid transporter and named LHT1 (Chen and Bush, 1997). Multiple independent T-DNA insertions in *LHT1*, named *lht1-1* to *lht1-7*, showed similar defense phenotypes to *Pseudomonas syringae* infection and reduced sensitivity to toxic D-Ala (see Supplemental Figures 1A to 1D online), which confirms the connection between LHT1 and these phenotypes. Hereafter, *lht1* will be used to refer to the *lht1-1* mutant, except where noted otherwise.

Initially, we thought that the accelerated leaf chlorosis in the *lht1* T-DNA insertion mutants was due to enhanced disease susceptibility. We thus further examined the detailed response of *lht1* to various *P. syringae* pv *tomato* strains, including virulent DC3000 (*PstV*), avirulent DC3000 harboring *avrRpt2* (*PstA*), and type III secretion system-defective *Pst hrcC*. Unexpectedly, we found that the stronger leaf chlorosis in the *lht1* mutant was associated with enhanced disease resistance rather than susceptibility. After inoculation with the virulent strain, bacterial proliferation in the mutant was 4- and 2-fold less than in the wild-type plant at 2 and 5 d after inoculation (DAI), respectively (Figure 1A). We also noticed significantly less growth ( $P < 0.05$ ) in the mutant at 2 DAI, but not 5

DAI, relative to the avirulent strain (Figure 1A). These tests were conducted with three biological repeats and multiple technical replicates at each repeat, and all results showed a similar trend. No significant difference in terms of bacterial growth was found between the wild type and the *lht1* mutant in response to *Pst hrcC*, even although this strain was inoculated at a higher titer than the other two strains as done in a previous study (Navarro et al., 2008) due to its slow growth. *Pst hrcC* carries a deletion in the *hrcC* gene that encodes a component of the type III secretion system (Wei et al., 2000) and is defective in delivering type III virulence effectors into host cells. This strain still triggers pattern-triggered immunity and hence serves as a useful control for examining basal defense response in plant cells. Interestingly, when callose deposition, a sensitive cellular marker for basal defense responses (Hauck et al., 2003), was investigated, *lht1* plants infected with each of the three *Pst* strains exhibited enhanced callose accumulation compared with their wild-type counterparts (Figure 1B). Although growth of the *hrcC* strain was dramatically reduced in comparison to a virulent *Pst* strain (Figure 1A), no significant difference was observed between wild-type and *lht1* plants. However, we observed more big callose depositions (Ham et al., 2007) in *lht1* mutants than in wild-type plants.

Extending this analysis, we further tested the mutant for resistance to the hemibiotrophic fungus *Colletotrichum higginsianum* (anthracnose pathogen; *Ch*) and the biotrophic fungus *Erysiphe cichoracearum* (powdery mildew; *Ec*). Compared with wild-type plants, the mutant displayed less fungal growth and fewer symptoms when infected with *Ch* and *Ec* (Figures 1C to 1E). Notably, this resistance was not because of pathogen penetration failure in the mutant but appeared to be due to enhanced host defense responses associated with host cell death, as revealed by nuclear condensation in *Ch*-infected epidermal cells, and tissue collapse, which correlated with callose deposition beneath the mildew-infected sites (see Supplemental Figures 2A and B online). Thus, disruption of the single amino acid transporter *LHT1* promoted postinvasion resistance to a broad spectrum of pathogens, likely by promoting hypersensitive cell death.

### Pathogen Infection Activates *LHT1* Expression

To further examine the involvement of *LHT1* in susceptibility, the levels of *LHT1* transcripts in wild-type plants were monitored following pathogen attack. The accumulation of *LHT1* transcripts was substantially induced after inoculation with either bacterial or fungal pathogens (Figure 2A). Additional evidence was obtained with reporter expression assays using *LHT1<sub>pro</sub>-GUS* (for  $\beta$ -glucuronidase). GUS staining was tightly associated with the site of pathogen infection in all three pathosystems, *Pst* (Figure 2B), *Ec* (Figure 2C), and *Ch* (Figure 2D). With *Ch* or *Ec* fungal infection, expression was found not only in the infected leaf epidermal cells but also in the uninfected mesophyll cells beneath the surface. In addition, the reporter was expressed at high levels in roots, pollen, and vascular strands of noninoculated plants (see Supplemental Figures 3A to 3G online), reflecting the important housekeeping function of *LHT1* (Hirner et al., 2006).

There are eight *LHT1*-like genes in the *Arabidopsis* genome (see Supplemental Figure 4A and Supplemental Data Set

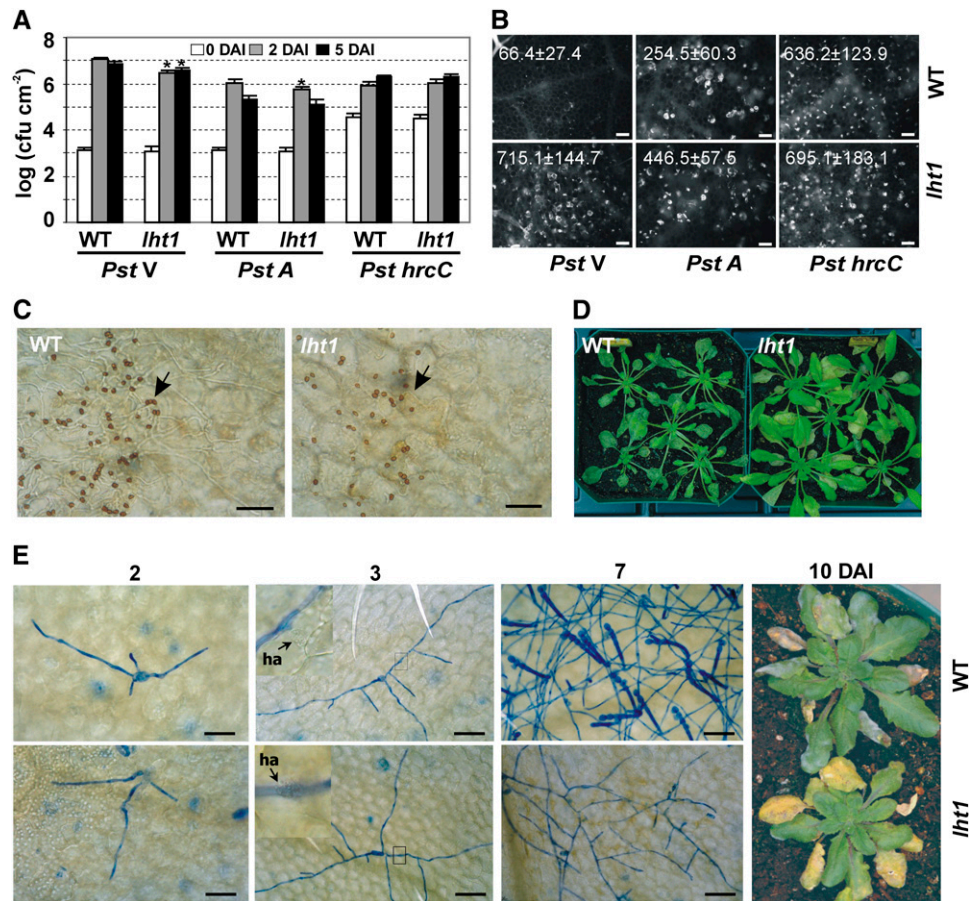


**Figure 1.** Enhanced Disease Resistance in *LHT1*-Knockout Lines to Different Pathogens.

**(A)** and **(B)** Bacterial growth and callose deposition in the leaves of wild-type Col-0 (WT) and the *lht1* mutant after infiltration with virulent (*Pst V*,  $10^5$  cfu mL<sup>-1</sup>), avirulent (*Pst A*,  $10^5$  cfu mL<sup>-1</sup>), and *hrp*-deficient (*Pst hrcC*,  $10^6$  cfu mL<sup>-1</sup>) strains, respectively.

**(A)** Bars represent mean values ( $\pm$ SD,  $n = 9$ ) of colony-forming units per square centimeter from three parallel samples each consisting of eight leaf discs. Asterisks denote pathogen growth with statistically significant differences between the wild type and *lht1* at the same time point within an individual strain ( $P < 0.05$ ; two-sided  $t$  test).

**(B)** The callose (white dots, strips, or circles) was stained with aniline blue and examined by epifluorescence microscopy 12 h after *Pst* infiltration. The number in each photograph indicates the average and SD of callose deposits per mm<sup>2</sup> leaf from seven independent leaves. Bars = 50  $\mu$ m.

**(C)** and **(D)** Cytological and symptomatic comparisons between the wild type and the *lht1* mutant at 4 DAI with fungal pathogen *Ch*. Arrows indicate the boundaries between inoculated and uninoculated areas. Bars = 50  $\mu$ m.

**(E)** Cytological and symptomatic comparisons between the wild type and the *lht1* mutant at 2 to 10 DAI with fungal pathogen *Ec*. The brownish color underneath the fungal infection sites indicates plant cells undergoing cell death. Insets show haustoria (ha; arrows) in epidermal cells and are enlargements of the boxed regions shown in the 3-DAI column. Bars = 50  $\mu$ m.

1 online). *LHT1* was constitutively expressed in all tissues, with the strongest signals in roots and leaves, whereas *LHT2* and *LHT3* showed strong signals in flowers and stems, respectively (see Supplemental Figure 4B online). However, none of these *LHT1*-like genes was induced by pathogen infection (see Supplemental Figure 4C online), suggesting that *LHT1* plays a unique role in the response to pathogen attack.

#### The *lht1*-Conferred Phenotypes Are SA-Dependent

We employed a set of mutant or transgenic plants defective in the SA, jasmonic acid (JA), or ethylene (ET) pathways to examine the

impact of these mutations on *LHT1* expression and function (see Supplemental Figure 5 online). Induction of *LHT1* by pathogen infection was greatly reduced in SA-associated *NahG* (transgenic plants harboring salicylate hydroxylase gene *NahG*) and *pad4-1* (*phytoalexin deficient 4*) plants, especially after inoculation with *Ec*, in contrast with the JA- or ET-defective mutants, *jasmonate resistant1* (*jar1-1*), *ethylene insensitive 2* (*ein2-1*), and *ethylene responsive1* (*etr1-1*). We further analyzed the effect of these pathways on disease resistance of *lht1* by creating double mutants. Double mutants of *lht1* and SA-associated pathway genes (i.e., *nonexpressor of pathogenesis-related protein1* [*npr1-3*], *SA induction deficient 2* [*sid2-1*], *pad4-1*, or *NahG*) were as

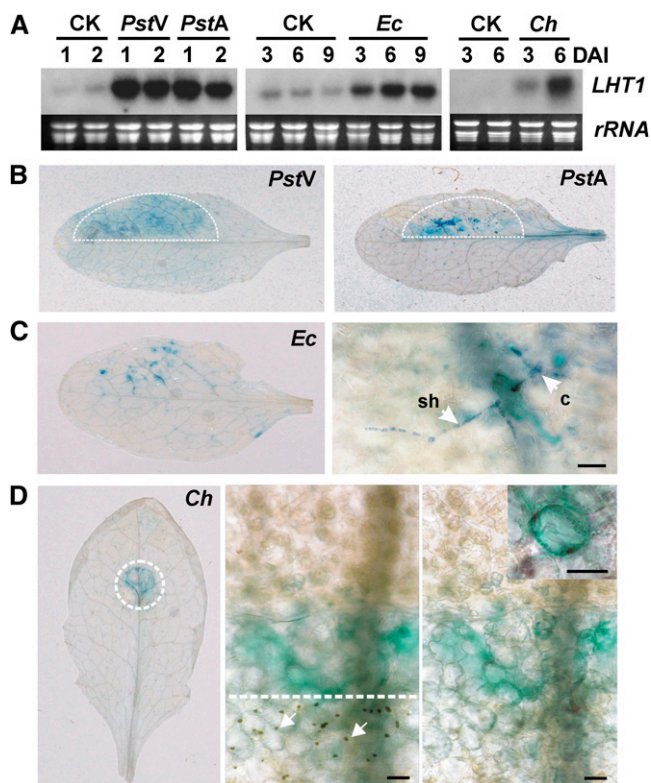


**Figure 2.** Pathogen-Induced *LHT1* Expression.

(A) RNA gel blot analysis of *LHT1* expression in the wild type in response to pathogen infections before (CK, mock control) and after different pathogen attack.

(B) to (D) *LHT1* promoter-driven GUS activity in response to pathogen infection. The inoculation boundary is outlined with dotted lines.

(B) GUS staining of leaves at 3 DAI with *PstV* (left) and *PstA* (right).

(C) GUS localization in leaf tissues at 4 DAI with *Ec*. Right panel shows a microscopic view of GUS activity associated with *Ec* infection. Arrowheads indicate conidia (c) and secondary hyphae (sh).

(D) GUS localization in leaf tissues at 2.5 DAI with *Ch*. The edges of inoculation sites were examined with a light microscope. The middle and right panels show the inoculated leaf surface and the mesophyll cell layer, respectively. Inset depicts an enlarged mesophyll cell. Arrows indicate melanized appressoria. Bars = 50  $\mu$ m.

sensitive as the respective single SA mutant in response to *Ec* or *Ch* infection. By contrast, mutations in the JA (*jar1*) or ET (*ein2*) pathway or in an aminotransferase (*ald1*, *AGD2-like defense response protein1*) (Song et al., 2004) did not diminish the enhanced resistance that was attributable to the *lht1* mutation (Figure 3A). *PR1* expression is a hallmark of the SA pathway. The *lht1* single mutant showed constitutive expression of *PR1*, whereas the double mutants affected in the SA pathway were compromised in both constitutive and pathogen-induced expression of *PR1* (Figure 3B), consistent with the disease phenotypes noted above. The *lht1 npr1* double mutant showed an intermediate level of *PR1* transcript after pathogen attack, supporting the hypothesis that SA-dependent, *NPR1*-independent *PR1* expression pathways exist.

The link between *LHT1* activation and the SA pathway was also supported by the rapid induction of *LHT1* transcripts in response to SA treatment (Figure 3C). The observation that *LHT1* expression was induced within 1 h of SA treatment suggests the presence of a positive feedback regulation loop by SA, as proposed for many well-known positive defense regulators, including *NPR1*, *PAD4*, or *ENHANCED DISEASE SUSCEPTIBILITY1* (*EDS1*) (Shah, 2003). However, the transcriptional induction of *LHT1* by SA suppresses plant defense reactions, which is in contrast with *NPR1* or *PAD4*, whose enhanced expression by SA promotes SA-dependent defense responses. Furthermore, SA application caused severe leaf chlorosis in *lht1*, *lht1 ein2*, *lht1 jar1*, and *lht1 ald1* plants, weak chlorosis on *lht1 pad4*, *lht1 sid2*, and *lht1 npr1* plants, and none on *lht1 NahG* plants (Figure 3D), suggesting that knockout of *LHT1* promoted the biosynthesis of and/or hypersensitivity to SA. Notably, the *lht1* mutant accumulated more SA than did the wild type, both before and after pathogen (*Pst*) attack (Figure 3E). Collectively, these results demonstrate that *LHT1* negatively modulates defense responses by interacting with the SA-dependent pathway.

#### The *lht1* Phenotypes Are Associated with Altered Redox Status

The *lht1* mutant displayed accelerated leaf senescence (Svennerstam et al., 2007). Particularly when grown under a long photoperiod (16 h), early senescence was exclusively associated with old leaves, and the senescing leaves showed an enhanced oxidative burst, as detected by 3,3-diaminobenzidine (DAB) staining (see Supplemental Figures 6A to 6D online). Interestingly, this *lht1*-associated early senescence could be efficiently suppressed when the SA pathway was perturbed by *NahG*, *pad4*, *sid2*, or *npr1* mutations (Figure 4A), and this senescence suppression pattern resembled the disease responses in the *lht1 NahG*, *lht1 pad4*, *lht1 sid2*, and *lht1 npr1* double mutants (Figure 3A). Considering that the suppression of the senescence and defense responses in *lht1* mutants depends on a light/SA-associated redox imbalance, we tested if the accelerated cell death observed in *lht1* mutants during pathogen attack was linked to redox status. Two major cellular redox intermediates,  $H_2O_2$  and nitric oxide (NO), were monitored in leaf tissues during the infection time course.  $H_2O_2$ -specific DAB coloration was always evident in the *Ec*-infected epidermal cells housing the primary haustoria and in the mesophyll cells beneath them in the *lht1* mutant, but only occasionally in the wild type (Figure 4B). Confocal imaging showed that  $H_2O_2$  and NO, detected by 2,7'-dichlorodihydrofluorescein diacetate (DCF-DA) and diaminofluorescein diacetate (DAF-DA), respectively, accumulated both in the apoplasts and chloroplasts of mildew infection-associated mesophyll cells in *lht1* plants (Figure 4B). The NO signal was also highly conspicuous in the nuclei (see Supplemental Figure 7 online). Notably, the accumulation of  $H_2O_2$  and NO in the mesophyll overlaps spatially with pathogen-induced *LHT1<sub>pro</sub>*-GUS reporter expression, indicating that *LHT1* activity might prevent the redox balance from shifting to the oxidative state, especially in photosynthetic tissues.

The biological redox relay network is very complex (Mittler et al., 2004; Foyer and Noctor, 2005). We adopted a genetic approach to investigate the role of *LHT1* in the biological redox

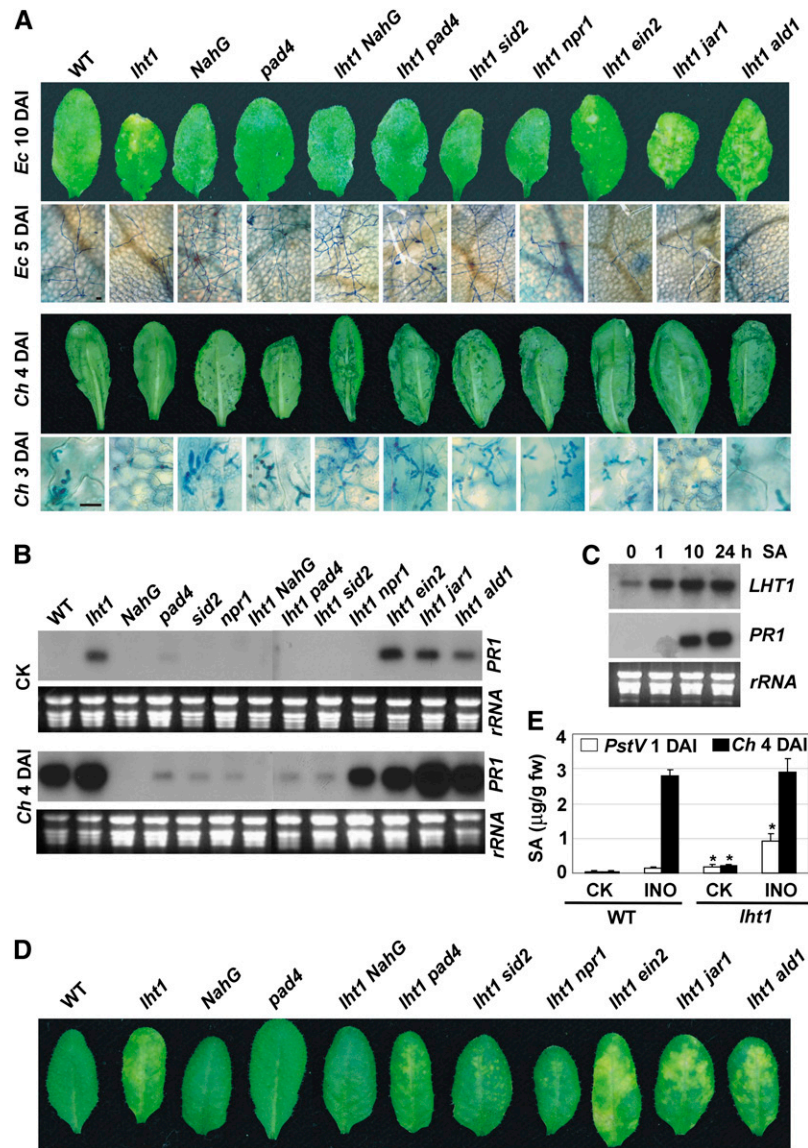


**Figure 3.** Genetic Dissection on *LHT1*-Associated Defense Pathways.

**(A)** Disease tests for single and *lht1*-related double mutants. Four-week-old plants (grown in short-day conditions) were inoculated with pathogens (*Ec* and *Ch*) and photographed at the indicated time points. The disease phenotypes are shown with representative leaves of the inoculated plants. Pathogen development in these inoculated leaves was monitored using aniline blue staining for *Ec* and trypan blue staining for *Ch*, as shown beneath the images of the corresponding diseased leaves. Bar = 50  $\mu$ m. WT, wild type.

**(B)** RNA gel blot analysis of *PR1* expression in mutants before (CK) and after pathogen infection.

**(C)** RNA gel blot analysis of *LHT1* transcript in response to treatment with 1 mM SA.

**(D)** In planta sensitivity of double mutants to SA-induced chlorosis. The leaves were photographed 7 d after spray with 2 mM SA.

**(E)** Free SA concentrations before (CK) and after (INO, inoculated) pathogen infections (mean  $\pm$  SD;  $n = 3$ ). Asterisks indicate that the SA concentration in *lht1* plants is statistically different ( $P < 0.05$ ; two-sided *t* test) from that in the corresponding wild-type plants. fw, fresh weight.

relay network. We generated double mutants consisting of *lht1* and *pad2* ( $\gamma$ -glutamylcysteine synthetase) (Parisy et al., 2007), which affects GSH metabolism by decreasing GSH biosynthesis; *rbohD* (*respiratory burst oxidase homolog D*) (Torres et al., 2002), which decreases NADPH oxidase activity and thereby affects the production of reactive oxygen species (ROS) in the plasma

membrane; *apx1* (*ascorbate peroxidase*) (Davletova et al., 2005), which affects the metabolism of hydrogen peroxide ( $H_2O_2$ ) in the cytoplasm; or *nudt7* (*Nudix hydrolase homolog 7*) (Bartsch et al., 2006; Ge et al., 2007), which affects NADH hydrolysis, perturbing cellular redox homeostasis and resulting in a higher level of NADH in pathogen-challenged leaves. None of these four

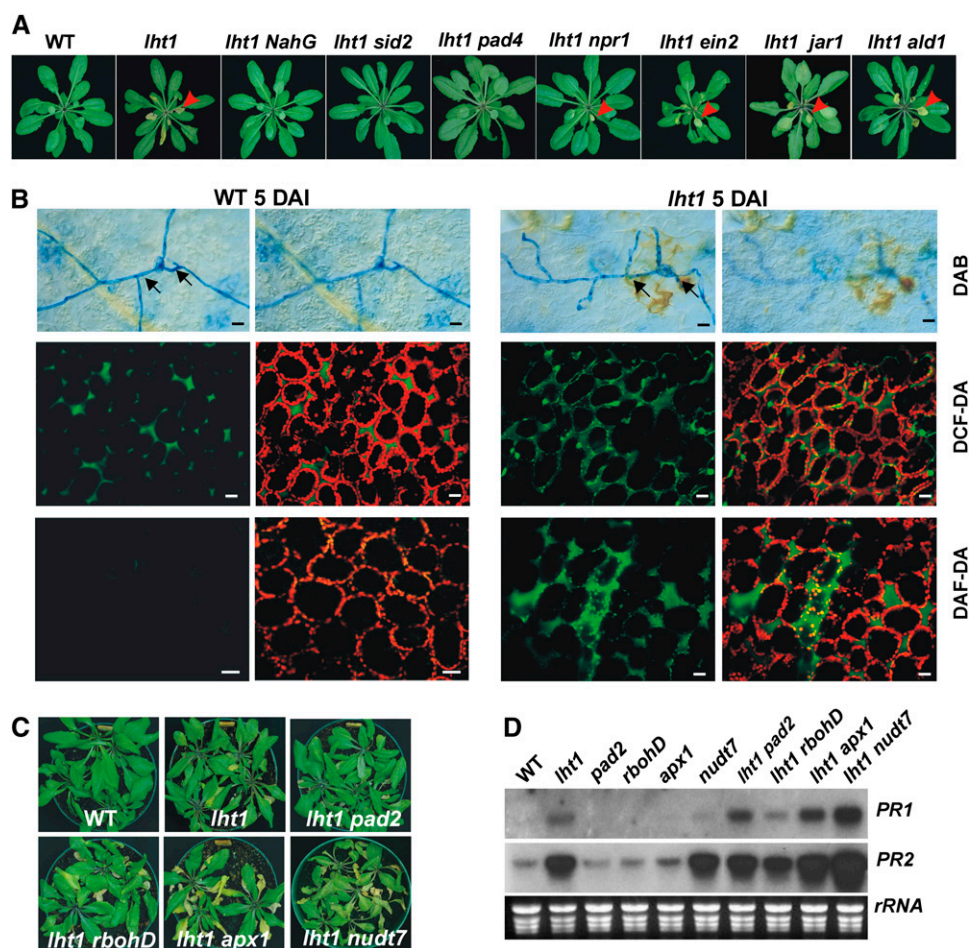


**Figure 4.** *lht1*-Associated Cell Death Is Linked to Redox Homeostasis.

**(A)** *lht1*-associated leaf senescence in long-day conditions. Representative plants were cut and photographed from the reverse side of a rosette to easily see the chlorotic leaves (red arrowheads). WT, wild type.

**(B)** Enhanced  $H_2O_2$ /NO production in *lht1* plants after pathogen infection. Top panels:  $H_2O_2$  accumulation (brownish signal), as detected by DAB staining. Arrows indicate fungal *Ec* penetration sites. Middle and bottom panels: Confocal images of mesophyll cells underneath the mildew-infected sites, showing  $H_2O_2$ -derived (green) or NO-sensitized (green) fluorescence with DCF-DA and DAF-DA, respectively, and their merged signals (yellow) of  $H_2O_2$ -derived or NO-sensitized fluorescence with chlorophyll autofluorescence (red), respectively. Bars = 20  $\mu$ m.

**(C)** Phenotypes of accelerated senescence in redox-related double mutants.

**(D)** Differential *PR* gene activation in redox-related single and double mutants.

mutations alone had a visible senescence-associated effect on plants, even when grown under 16-h light conditions. However, the double mutants *lht1 apx1* and *lht1 nudt7* displayed stronger senescence phenotypes than did the single *lht1* mutant (Figure 4C). By contrast, *lht1 rbohD* and *lht1 pad2* plants did not exhibit such developmental differences compared with *lht1* plants. However, the *lht1 pad2* double mutant showed a water soaking-like leaf chlorosis. We assayed *PR* expression in all of these double mutants and found synergetic induction of *PR1* and *PR2*, particularly in *lht1 nudt7* (Figure 4D). Thus, these results show that the *APX1*-, *PAD2*-, *RBOHD*-, and *NUDT7*-dependent cellular redox pathways intersect, albeit to various extents, with the *LHT1*-associated redox regulation that leads to developmental and defense responses.

#### Microarray Analysis Links LHT1 to the Defense Response, Cellular Redox, and Nitrogen Metabolism

To gain an overview of the global gene expression profile in *lht1*, we analyzed its transcriptome using ATH1 Affymetrix chips. Briefly, we found that 1140 and 1204 genes were up- and downregulated, respectively, in wild-type plants upon infection with *Pst* DC3000 when compared with noninoculated wild-type plants, whereas in uninfected *lht1*, 3298 and 3082 genes were up- and downregulated compared with noninoculated wild type. Thus, *lht1* was more active than virulent *Pst*-challenged wild type at aspect of differential gene expression. However, there was a substantial correlation in gene expression changes between *lht1* and wild-type plants in response to pathogen challenge (see

Supplemental Figure 8 online). Functional classification established that 875 genes were upregulated both in the infected wild type and in the uninfected *lht1* mutant. These genes included genes associated with defense pathways and redox homeostasis. Table 1 highlights some of these genes. Although this list is not comprehensive, it does illustrate that patterns of gene expression in uninfected *lht1* plants mimic those in infected wild-type plants. Notably, chorismate and the downstream Phe, Trp, and SA metabolism-related genes, systemic acquired resistance-associated *ALD1* (Song et al., 2004), and redox homeostasis- and defense-associated genes, *FMO* and *NUDT* (Bartsch et al., 2006), were among the most upregulated genes in the *lht1* mutant (Table 1, Figure 5A). Among the most downregulated genes in *lht1* were ERF/AP2 (ethylene responsive factor/activator protein-2) transcription factors and auxin (indole-3-acetic acid)-responsive proteins, which in part reflects the antagonistic effect between SA and those pathways.

Common marker genes for sensing intracellular N deficiency, including two major inorganic N ( $\text{NO}_3^-$  and  $\text{NH}_4^+$ ) transporters, *NRT1* and *AMT1*, were also strongly upregulated in *lht1* (Table 1). The photorespiration pathway genes were downregulated in *lht1* (Figure 5A), suggesting that the coordination of redox balance and  $\text{NH}_4^+$  reutilization in green tissues was affected in the mutant. These results led us to reassess if the enhanced defense reactions in the *lht1* mutant merely rely on a general N deficiency. To test this, we compared the defense responses of a well-characterized inorganic N-deficient double mutant, *nia1 nia2* (Wilkinson and Crawford, 1993), with those of *lht1* and a triple mutant, *lht1 nia1 nia2*, that we generated and confirmed by sequencing. Both *nia1 nia2* and *lht1 nia1 nia2* plants exhibited the typical general N deficiency phenotype (small and yellowish plants). The double *nia1 nia2* mutant did not exhibit enhanced *PR1* expression or have altered resistance to infections by *Ec*

and *Ch* compared with wild-type plants; therefore, a general N deficiency does not impact disease resistance (Figure 5B). Not surprisingly, this general N deficiency did not promote the disease resistance phenotype of *lht1*, as observed in the *lht1 nia1 nia2* triple mutant. Therefore, despite the fact that the status and location of different N forms are tightly correlated in plant cells (Coruzzi, 2003), it appears that elevated resistance in *lht1* is not directly linked to inorganic nitrogen assimilation and the associated general N status.

### Gln Is One of the Main Physiological Substrates of LHT1

To analyze the metabolic nature of the enhanced defense response in *lht1* leaves, we profiled free amino acids in plants subjected or not to powdery mildew attack (Figure 6A). Among the 16 amino acids detected in our method, the most abundant were Gln, Glu, Asp, and Ser, which together accounted for 64.3 and 64.9% of the total amount of amino acids present in the wild type and *lht1*, respectively. Gln, Ala, and Pro contents were significantly lower ( $P < 0.05$ ) in *lht1* than in wild-type plants. The mutant showed a tendency to have lower levels of other amino acids also, reflecting a general deficiency of free amino acids in the *lht1* mutant. Notably, the amino acid depletion was also observed in wild-type plants after pathogen infection, which exhibited a significant ( $P < 0.05$ ) decrease in Gln, Gly, and Pro. Interestingly, large changes of free amino acids in wild-type plants, particularly of Gln levels, occurred at 3 DAI, and no further significant decrease was detected at 9 DAI, indicating that host cellular Gln depletion occurs soon after infection and does not coincide with the pathogen's heavy colonization. These data suggest that free amino acids, especially Gln, might be quickly drained from infection sites during the early infection process in the wild type, although this would be alleviated to some degree

**Table 1.** Examples of Defense/Redox- and N Metabolism-Associated Genes That Are Significantly Altered in the *lht1* Mutant Compared with the Wild Type

Locus	Annotation	Fold Change	P Value
At2g14610	<i>PR1</i> (Pathogenesis-Related Protein 1)	77.00	2.78E-09
At1g75040	<i>PR5</i> (Pathogenesis-Related Protein 5)	18.84	5.27E-07
At2g04450	<i>NUDT6</i> (Nudix Hydrolase Homolog 6)	15.15	1.43E-07
At1g19250	<i>FMO1</i> (Flavin-Dependent Monooxygenase 1)	13.21	9.01E-06
At4g39030	<i>EDS5</i> (Enhanced Disease Susceptibility 5)	6.71	7.29E-06
At1g02920	<i>GST11</i> (Glutathione S-Transferase 11)	5.83	1.43E-07
At1g74710	<i>EDS16</i> , <i>SID2</i> , <i>ICS1</i> (Isochorismate Synthase 1)	5.34	2.99E-05
At2g37040	<i>PAL1</i> (Phenylalanine Ammonia-Lyase 1)	4.77	4.94E-06
At4g12720	<i>NUDT7</i> (NAD/NADH Binding/Hydrolase 7)	4.56	1.49E-05
At5g44420	<i>PDF1.2</i> (Defensin 1.2)	4.37	0.005233
At3g52430	<i>PAD4</i> (Phytoalexin Deficient 4)	3.99	0.000352
At2g30770	<i>CYP71A13</i> (Cytochrome P450)	3.74	7.45E-08
At2g13810	<i>ALD1</i> (AGD2-Like Defense Response Protein1)	3.70	0.009679
At4g39950	<i>CYP79B2</i> (Cytochrome P450)	3.65	2.79E-05
At2g04430	<i>NUDT5</i> (Nudix Hydrolase Homolog 5)	3.50	7.48E-05
At3g48090	<i>EDS1</i> (Enhanced Disease Susceptibility 1)	3.16	0.002081
At3g53260	<i>PAL2</i> (Phenylalanine Ammonia-Lyase 2)	2.96	0.002286
At2g29470	<i>GST21</i> (Glutathione S-Transferase 21)	2.58	0.000141
At1g12110	<i>NRT1.1</i> (Nitrate Transporter 1.1)	2.43	2.18E-05
At1g64780	<i>AMT1;2</i> (Ammonium Transporter 1;2)	2.10	6.09E-06
At4g13510	<i>AMT1;1</i> (Ammonium Transporter 1;1)	2.02	1.34E-05

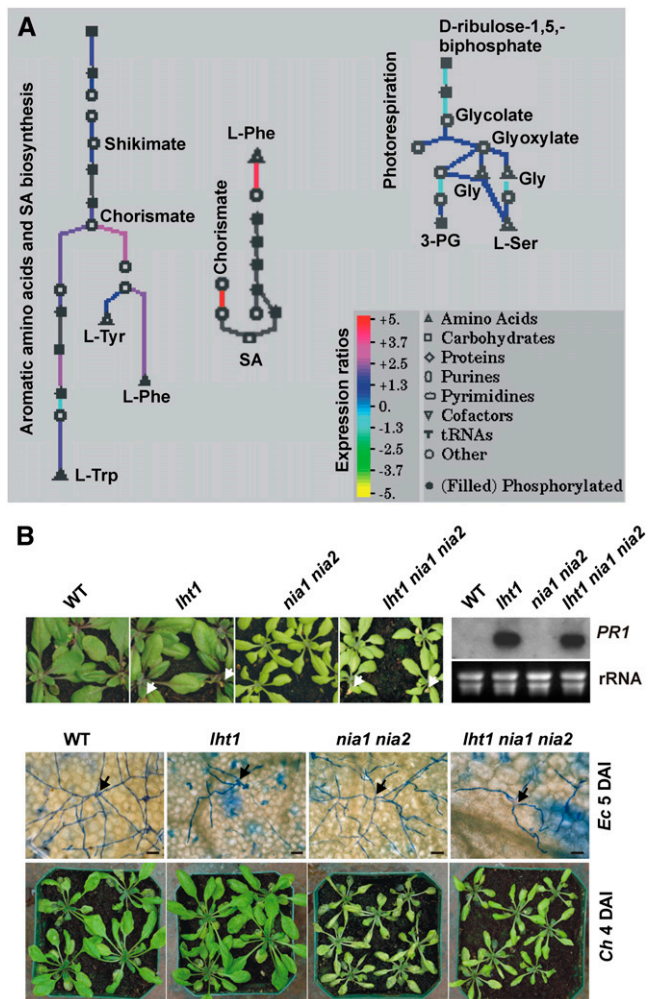


**Figure 5.** Distinctive Roles of Organic and Inorganic N Sources in Defense Responses.

**(A)** Ratio changes of gene expression of the *lht1* mutant versus the wild type in representative metabolic pathways, as illustrated using Omics Viewers (Pathway Tools version 12.5; expression ratios are within  $\pm 5$ -fold).

**(B)** Developmental phenotypes, constitutive *PR1* expression, and disease reaction of *nia1 nia2* double and *nia1 nia2 lht1* triple mutants compared with the wild type (WT) and *lht1* single mutant. White arrows indicate senescent leaves. Black arrows indicate germinated conidia 5 DAI with *Ec*. Bars = 50  $\mu\text{m}$ .

due to the presence of LHT1. Thus, the enhanced defense response in *lht1* mutant is likely due to altered amino acid homeostasis.

A question that now arises is which amino acid(s) transported by LHT1 plays the major role in suppressing defense responses. LHT1, initially defined as a Lys/His-specific transporter (Chen and Bush, 1997), was later reported to transport a broad spectrum of amino acids in a heterologous yeast expression system (Hirner et al., 2006). However, a recent report using an in planta approach with  $^{15}\text{N}$ -labeled amino acids demonstrated that LHT1

has a critical role in the uptake of L-Gln and L-Ala but not L-Lys (Svennerstam et al., 2007). In view of these contradictory results, we adapted an assay that uses D-enantiomeric amino acids (Erikson et al., 2004). D-enantiomers are generally toxic to plant cells but are thought to be taken up by the same transporters and with similar kinetics as their L-form counterparts (Erikson et al., 2004; Svennerstam et al., 2007; Forsum et al., 2008). Our results showed that, although both *lht1* and wild-type seeds germinated well on complete Murashige and Skoog (MS) medium supplemented with a range of concentrations of D-amino acids, except for D-Cys, significant inhibition of root and leaf development were observed, indicating that all tested D-enantiomers are toxic to *Arabidopsis* (see Supplemental Figure 9 online). Interestingly, the root growth of both the wild type and *lht1* was inhibited equally by all D-enantiomers, except by D-Gln and D-Asn, which inhibited the wild type to a greater degree than it did the *lht1* mutant. To further validate this specific inhibition, we used D-enantiomers of Glu, Gln, Asp, or Asn as the sole N source in the germination assay. Consistently, root development was more sensitive to inhibition by D-Gln and D-Asn in the wild-type plants than in the *lht1* plants (Figure 6B). Given that free Gln is the most abundant amino acid in planta and that it is the amino acid that is most significantly changed in both the *lht1* mutant and in pathogen-infected wild-type plants, Gln might be one of the main physiological substrates of LHT1. We therefore examined this possibility in further studies.

### A Gln Deficiency Is Correlated with Activation of Defense Responses

We used the following genetic and pharmacological approaches to validate the involvement of Gln in disease resistance. The *Arabidopsis* mutant *gdu1-1D* specifically expels Gln from cells on the leaf edges (Pilot et al., 2004). Interestingly, we found that the leaves of this Gln dumper mutant showed spontaneous lesion-mimic when Gln hypersecretion from hydathodes was conspicuous (Figure 7A).  $\text{H}_2\text{O}_2$  and callose accumulated in the lesions (Figures 7B and 7C). The expression of *PR1*, as well as of *LHT1*, was highly activated in the leaves. The ammonium transporter gene *AMT1;1* has been used as a molecular probe for sensing the N status, and its expression is specifically induced by cytosolic Gln depletion (Rawat et al., 1999). Expression of *AMT1;1* was constitutively activated in both the *gdu1* and *lht1* mutants, suggesting that Gln is deficient in the leaf tissues of these mutants (Figure 7D). Not only did the *gdu1* plant display the hallmarks of the activated defense response, such as enhanced ROS production and *PR1* accumulation, but it also exhibited strong disease resistance, similar to *lht1*, in the form of post-invasion-associated cell death and pathogen arrest (Figure 7E).

Pharmacological intervention of Gln synthesis in wild-type plants also confirmed the involvement of Gln depletion in the plant defense response. Direct Gln administration onto leaves resulted in strong inhibition of  $\text{H}_2\text{O}_2$  production (see Supplemental Figure 10A online). The herbicide L-PPT (L-phosphinothricin or glufosinate), a potent inhibitor of GS, caused leaf chlorosis within three to 4 d of application (see Supplemental Figure 10B online). Coadministration of Gln and L-PPT alleviated the chlorosis symptoms in proportion to the Gln concentration used



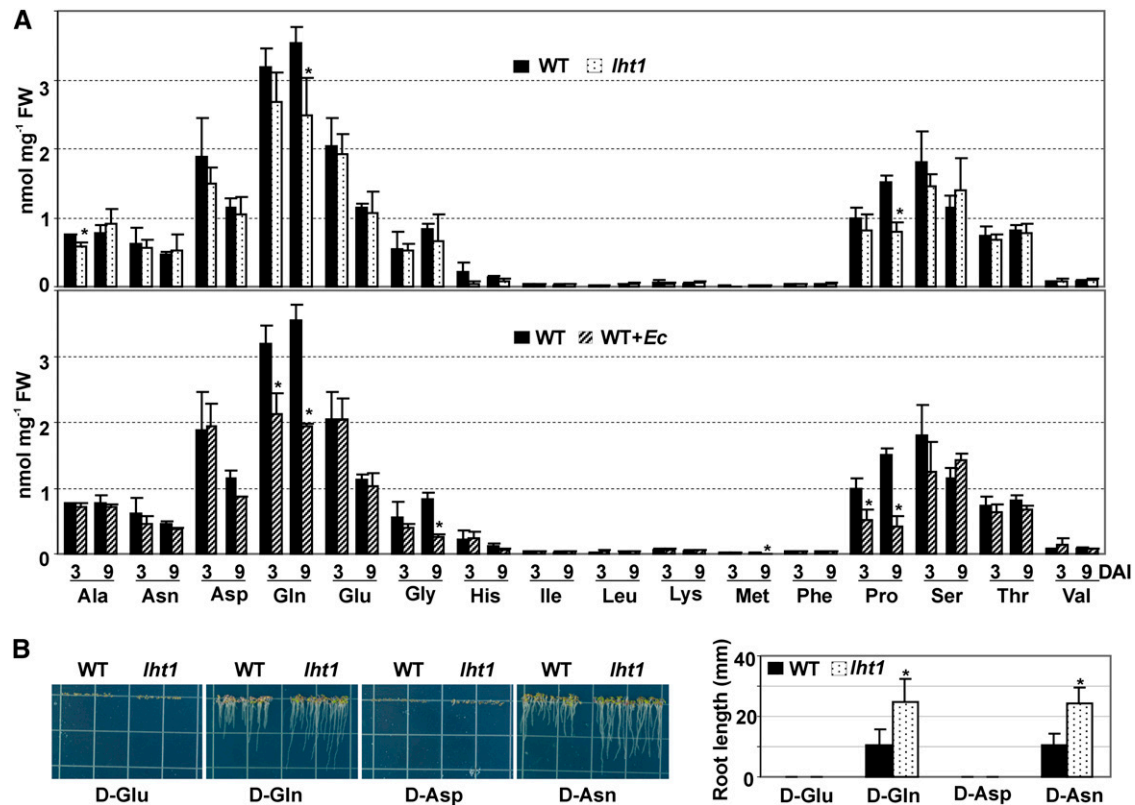


**Figure 6.** Alterations in Amino Acid Homeostasis in *lht1* Mutant and Its Tolerance to D-Amino Acids.

**(A)** Free amino acid profiling in the wild type (WT) versus *lht1* leaf tissues (top panel) and in the wild-type leaf tissue of plants inoculated or not with *Ec* (bottom panel). The bar values represent means  $\pm$  SD ( $n > 3$ ). Asterisks indicate a statistically significant difference ( $P < 0.05$ ; two-sided  $t$  test) of uninoculated *lht1* (top panel) or inoculated wild type (bottom panel) compared with the wild type. FW, fresh weight.

**(B)** Root growth phenotypes of the wild type and *lht1* mutant in MS-N medium supplemented with 3 mM D-Glu, D-Gln, D-Asp, or D-Asn as sole N source. The seeds were pretreated at 4°C for 3 d before being moved to room temperature. Seedlings were photographed at 5 d after germination. Root length was measured (right graph), and the bar values represent means  $\pm$  SD ( $n > 20$ ). Asterisks indicate statistically significant differences ( $P < 0.05$ ; two-sided  $t$  test) compared with the wild type.

[See online article for color version of this figure.]

(see Supplemental Figure 10C online), indicating the specificity of Gln biosynthesis inhibition by L-PPT. Transcription of *PR1* and *AMT1;1* was upregulated in response to the L-PPT treatment (Figure 7F). Thus, L-PPT-provoked *PR1* gene expression (Ahn, 2008) is due to the endogenous depletion of Gln.

We also showed that pathogen attack promoted intracellular Gln depletion in host cells. Induction of *AMT1;1* expression was noticeable upon either bacterial (*PstV*) or fungal (*Ec*) attack (Figure 8A). *AMT1;1* accumulation was also specifically observed in *Ec* infection-associated host cells expressing an *AMT1;1<sub>pro-AMT1;1</sub>-GFP* (for green fluorescent protein) construct (Figure 8B).

Finally, we demonstrated that the inhibition and degradation of GS enzymes contributed to intracellular Gln depletion in the host during pathogenesis. The GS proteins were degraded by 6 d after *Ec* infection; however, the degradation was largely attributed to the plastidic isoform, GS2, rather than to cytosolic GS1 (Figure 8C), as revealed in other pathosystems (Perez-Garcia et al., 1995, 1998; Pageau et al., 2006). We repeatedly detected

similar GS degradation patterns during infection processes by immunoblot analysis of crude leaf extracts from intact leaf tissues; however, cleaved fragments of GS2 were not present in chloroplast lysates when the same leaf materials were used for chloroplast preparation, suggesting that the hydrolyzing process outside the plastid might be responsible for the degradation of GS2. Recent studies demonstrated that senescence-associated vacuoles are involved in the degradation of chloroplastic proteins, including GS2, the large subunit of ribulose-1,5-bis-phosphate carboxylase/oxygenase, and other soluble photosynthetic proteins of the chloroplast stroma during leaf senescence (Feller et al., 2008; Martínez et al., 2008). We propose that an extraplastidic pathway involving senescence-associated vacuoles might participate in the degradation of plastidic GS proteins during pathogen infection.

Although protein degradation was evident at 6 DAI, significant inhibition of GS activity in either whole leaves or chloroplast proteins occurred as early as at 3 DAI (Figure 8D). Note that, at 3 DAI, there is no massive fungal colonization, chlorophyll

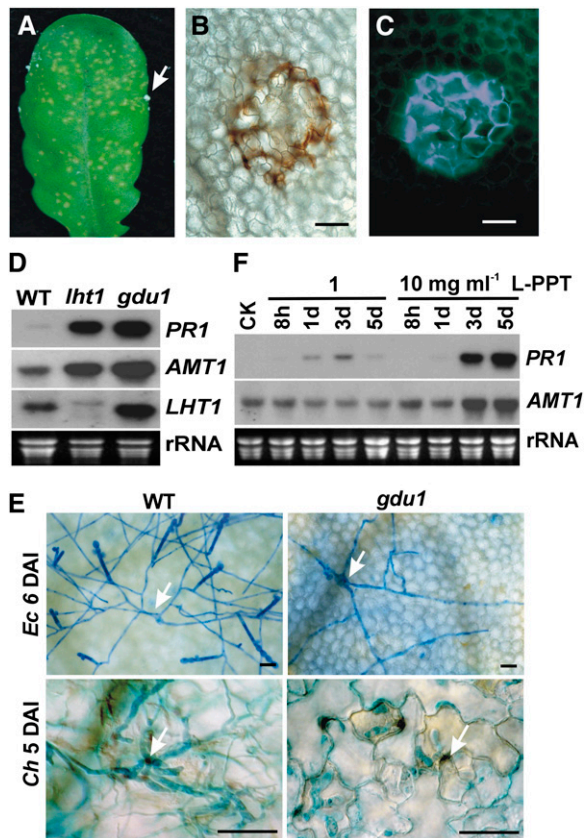


**Figure 7.** Gln Deficiency Underlies Defense Responses.

**(A)** Spontaneous lesion formation in the Gln-deficient *gdu1* mutant. Arrow indicates Gln-enriched crystals secreted through the hydathode. **(B)** and **(C)** Lesion-associated  $H_2O_2$  production, as detected by DAB staining **(B)** and callose deposition **(C)** in the *gdu1* mutant. Bars = 50  $\mu$ m. WT, wild type.

**(D)** Constitutive activation of *PR1*, *LHT1*, and *AMT1;1* genes in the *gdu1* mutant.

**(E)** Compromised fungal development in the *gdu1* mutant after inoculation with *Ec* and *Ch*. The hyphae were stained with aniline blue (top panels) and trypan blue (bottom panels), respectively. Arrows indicate conidia. Bars = 50  $\mu$ m.

**(F)** L-PPT application induces *PR1* and *AMT1;1* gene expression. CK, control.

[See online article for color version of this figure.]

degradation, or nutrient deprivation. Thus, inhibition of GS2 activity occurred before GS2 degradation during the infection process. It is unlikely that a nonspecific cellular protein remobilization process contributed to the reduction in GS2 activity during the early stages of infection with a lower density inoculation (5 to 10 conidia  $mm^{-2}$ ) of *Ec* than that used in a normal inoculation (20 to 50 conidia  $mm^{-2}$ ). Whereas the SDS-PAGE analysis of crude extracts of leaf tissues showed no distinct changes in protein profiling between noninfected and infected leaves, regardless of the infection time points (3 or 6 DAI) (Figure 8C), it is possible that GS2 protein degradation at later stages of pathogen infection (6 DAI) might be due in part to a senescence

remobilization process. SDS-PAGE analysis of chloroplast lysates extracted from the same leaf materials revealed dramatic changes in chloroplastic protein dynamics during the infection process. Chloroplastic protein turnover, which includes elimination of GS2 activity, might be involved in the early stages of host response against pathogen infection.

In agreement with GS protein stability being sensitive to oxidative stress (Ortega et al., 1999; Palatnik et al., 1999; Gómez-Baena et al., 2006), the GS activity in *Arabidopsis* leaves was inhibited by reactive oxygen or nitrogen species (Figure 8E), and ROS and NO exhibited an additive effect in this regard. These results suggest that the oxidative burst triggered by pathogen attack may lead to diminished GS2 activity and subsequently to Gln deficiency.

## DISCUSSION

### LHT1, an Important Amino Acid Transporter, Influences Plant Immunity

LHT1 was previously reported to be a basic amino acid transporter (Chen and Bush, 1997) and was recently shown to be involved in amino acid uptake in roots and in supplying leaf mesophyll with xylem-derived amino acids (Hirner et al., 2006; Svennerstam et al., 2007). Here, we show that *Arabidopsis* LHT1 acts as a novel modulator of the plant defense response. The pathogens suppress plant immunity by enhancing the expression of *LHT1* very early in the infection process, before the hallmark upregulation of *PR1*, supporting the claim that foliar pathogen-induced reprogramming of host metabolites occurs in presymptomatic tissues via active signaling, as proposed by Spanu and Kämper (2010). It is clear from elaborate genetic evidence that the SA pathway, but not the ET or JA pathway, is specifically and intriguingly co-opted for this induction. The *as1* element, a binding site for bZIP transcription factors that are essential for SA-induced gene expression, is present in the *LHT1* promoter (Liu and Bush, 2006). The *as1* element likely provides the physical link between SA signaling and regulation of amino acid transport. The increased level of SA in the *lht1* mutant is presumably due to the upregulation of chorismate/Phe metabolism-related genes, as seen in the microarray analysis (Figure 5A, Table 1). Thus, the perturbed amino acid homeostasis in the *lht1* mutant might in turn contribute to SA production/signaling. Whereas this study focused on the plant immune response to biotrophic/hemibiotrophic pathogens, we also tested the role of LHT1, if any, in the defense response against necrotrophic *Sclerotinia sclerotiorum*. The lack of any significant difference in disease development between the wild type and the *lht1* mutant reinforces the idea that *LHT1* is involved in SA-dependent defense.

In the absence of LHT1, the *lht1* plants became more resistant to a broad spectrum of pathogens. Enhanced resistance in *lht1* plants was associated with accelerated callose deposition,  $H_2O_2$ /NO accumulation, and programmed cell death at the site of pathogen challenge. The enhanced accumulation of  $H_2O_2$  and NO, two major cellular redox intermediates, in pathogen-infected epidermal cells and at the apoplast and chloroplast of the mesophyll cells of *lht1* plants resembled the expression

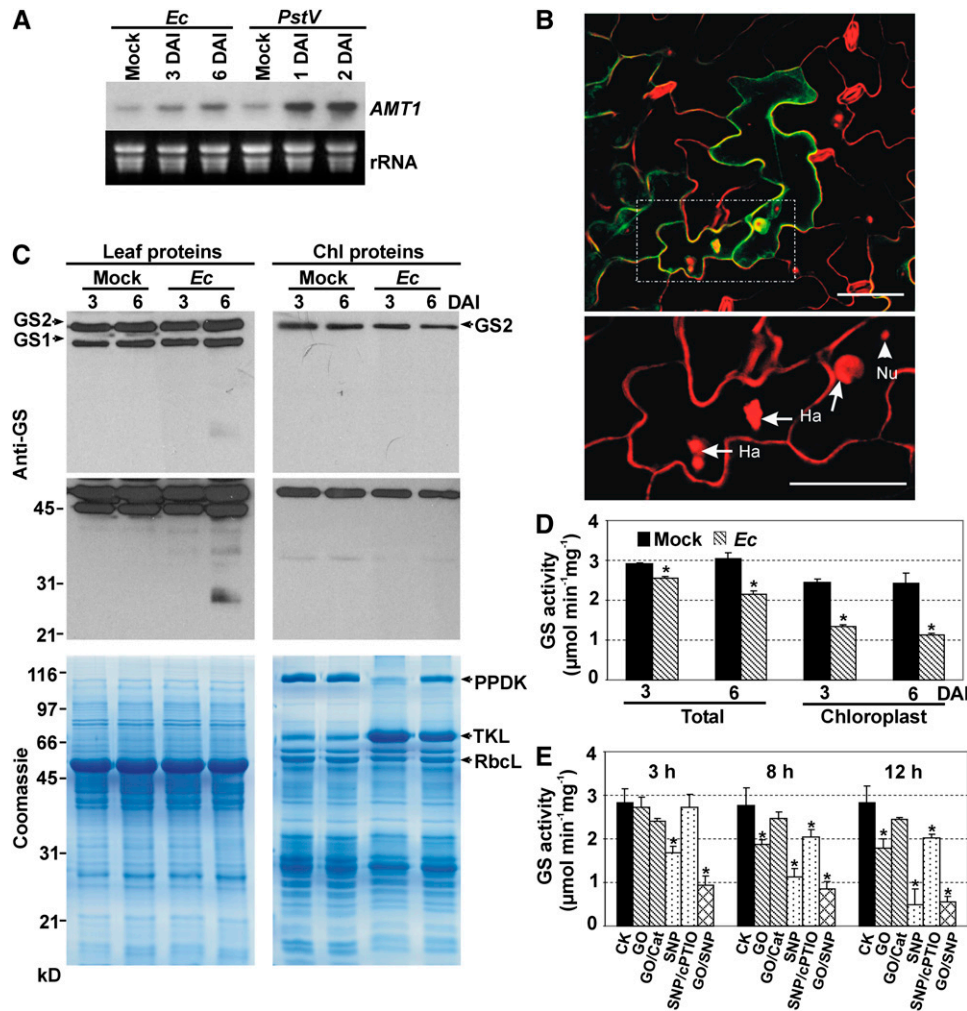


**Figure 8.** Pathogen Infection Induces a Gln Deficiency by Inhibiting GS2 Activity.

**(A)** RNA gel blot analysis of *AMT1;1* gene expression in response to pathogen infection (*Ec* and *PstV*) compared with uninfected plants (Mock).

**(B)** Pathogen infection-triggered accumulation of the *AMT1;1*-GFP fusion protein. GFP fluorescence (green) was detected in transgenic *AMT1;1<sub>pro</sub>*-*AMT1;1*-GFP *Arabidopsis* leaves by means of confocal microscopy at 3 DAI with *Ec*. Red fluorescence of PI was used to visualize plant cell walls, fungal haustoria (Ha), and the nucleus (Nu). Top panel, merged GFP/PI image; bottom panel, enlarged single PI channel image (the region is an enlargement of the boxed region shown in the top panel). Bar = 50  $\mu\text{m}$ .

**(C)** Pathogen infection-associated turnover of GS proteins as determined by immunoblot analysis. Total proteins were extracted from intact leaf tissues or chloroplasts (Chl) of leaves inoculated with *Ec*. The films of the same blot were exposed for different time periods (top and middle panels); the film in the middle panel was exposed for a longer period than was that in the top panel) to differentiate the dynamic changes between isoforms GS1 and GS2. The same amounts of proteins used for immunoblot were visualized by Coomassie blue staining (bottom panels). The abundant known marker proteins in chloroplasts are indicated. PPDK, pyruvate phosphate dikinase; TKL, transketolase; RbcL, ribulose-1,5-bisphosphate carboxylase/oxygenase large subunit.

**(D)** Total GS activity was suppressed after mildew infection. GS activities were measured from total proteins extracted from leaf tissues or isolated chloroplasts of wild-type *Arabidopsis* leaves 3 and 6 DAI with *Ec* or a mock inoculation. The bar values represent means  $\pm$  SD ( $n = 6$ ). Asterisks indicate statistically significant differences ( $P < 0.05$ ; two-sided  $t$  test) compared with the control.

**(E)** Total GS activities were inhibited by reactive oxygen/nitrogen species. Total leaf proteins were prepared at the indicated time points after infiltration with either single or combined compounds. GO, glucose oxidase ( $0.5 \text{ units mL}^{-1}$ ); Cat, catalase ( $300 \text{ units mL}^{-1}$ ); SNP, sodium nitroprusside ( $0.5 \text{ mM}$ ); cPTIO, 2-(4-carboxyphenyl)-4,4,5,5-tetramethylimidazole-1-oxyl-3-oxide ( $500 \mu\text{M}$ ). The bar values represent means  $\pm$  SD ( $n = 3$ ). Asterisks indicate statistically significant differences ( $P < 0.05$ ; two-sided  $t$  test) compared with the control (CK).

pattern of GUS driven by the native *LHT1* promoter, which establishes a correlation between the regulation of *LHT1* expression and changes in cellular redox homeostasis. Collectively, our data suggest that *LHT1* is an important modulator of plant immunity.

### The Plant Defense Response Appears to Be Suppressed by Gln, a Substrate of *LHT1*

Because pathogens require N from their hosts, the amount of N available to pathogens can alter the pathogenic outcomes of infection. Thus, although increased amounts of N are traditionally thought to render plants more susceptible to certain types of pathogens, including biotrophic rusts and powdery mildews, the underlying molecular mechanism remains unknown. The total soluble N pool appears to be abundant in leaves (millimolar level), but N availability might be generally limiting to pathogens (Snoeijers et al., 2000; Divon and Fluhr, 2007). Several reports showed that pathogens prefer specific amino acids to inorganic N (Hahn et al., 1997; Pellier et al., 2003; Solomon et al., 2003). It is possible that it is not the amount of N but the form of N that is available to the host or pathogen that affects disease susceptibility or resistance. In addition, N concentrations in the apoplast and symplast of the host tissue could be dramatically different, and some biotrophic pathogens can only absorb a cytosolic N source via haustoria or invasion vesicles (Solomon et al., 2003).

Our study provides compelling evidence that the depletion of cellular amino acids, rather than of inorganic  $\text{NH}_4^+$ , enhances host defense responses. We showed that total free amino acid levels were reduced in host tissues upon pathogen infection. In the *lht1* mutant, our microarray analysis suggested that amino acid depletion was accompanied by a cytosolic  $\text{NH}_4^+$  deficiency, which might also be associated with an accumulation of  $\text{NH}_4^+$  in the apoplastic fluid of *lht1* (Hirner et al., 2006). The fact that a nitrate reductase-null mutant, *nia1 nia2*, depleted in cellular  $\text{NH}_4^+$  levels showed similar levels of defense responses and disease severity to pathogen infection as did wild-type plants indicates that limiting cytosolic  $\text{NH}_4^+$  is an unlikely candidate for triggering host defense responses. The *lht1 nia1 nia2* triple mutant showed growth phenotypes similar to *nia1 nia2* plants but exhibited enhanced defense responses that resembled the *lht1* responses against pathogen infections, suggesting that N status in the form of amino acids influences host defense responses.

In *Arabidopsis* leaves, Gln, Glu, Asp, and Ser are the most abundant amino acids, accounting for 64.3% of the total amino acids present. Although *LHT1* was previously reported to be a broad-spectrum amino acid transporter (Hirner et al., 2006; Svennerstam et al., 2007; Forsum et al., 2008), these abundant amino acids are possibly the main physiological substrates of *LHT1*. Growth assays on D-amino acids as the sole nitrogen source showed that the root growth of the *lht1* mutant was less sensitive to the toxic D-Gln and D-Asn, suggesting that Gln and Asn are preferred substrates of *LHT1*. We focused on Gln in this study, and our conclusion that Gln deficiency plays a major role in enhanced defense responses of *lht1* plants, not necessarily to the exclusion of a similar role for Asn, was supported by the use of a well-characterized genetic mutant, *Glutamine dumper* (*gdu1*). This mutant showed massive Gln secretion at its leaf

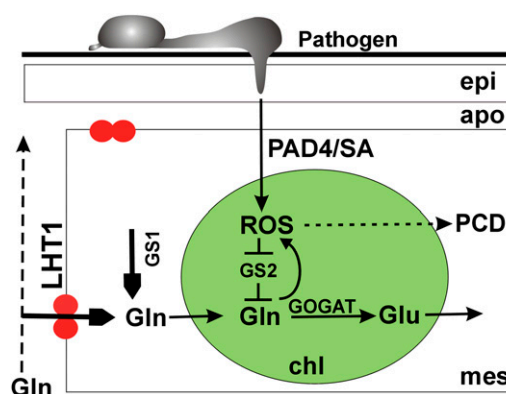


**Figure 9.** A Novel Role for the Gln Transporter *LHT1* in Defense Responses.

The model depicts the dynamic role of *LHT1* (red circles) and its substrate Gln in suppressing cell death during pathogen infection. epi, epidermal cell; apo, apoplast; mes, mesophyll cell; chl, chloroplast. [See online article for color version of this figure.]

margins (Pilot et al., 2004) and a depletion of cytosolic Gln, accompanied by hallmarks of activated defense responses and enhanced disease resistance. The appearance of smaller, chlorotic leaves in the double mutant *lht1 gdu1* indicates a possible synergistic effect between the lower uptake of Gln into and the enhanced secretion of Gln out of the leaf tissue (see Supplemental Figure 11 online). Additional support for this hypothesis was derived from pharmacological studies with glufosinate, which affects Gln synthesis.

Expression of *AMT1;1*, a molecular sensor of cytosolic Gln status (Rawat et al., 1999), was induced during pathogen attack, suggesting that the infected host cells have an underlying deficiency in Gln. The Gln depletion in infected host tissues might also be due to the specific acquisition and usage of amino acids by the pathogen, as revealed in human pathosystems (Hofreuter et al., 2008; Blume et al., 2009), although it appears that this direct pathogen drain might contribute only partially to this depletion, especially during the early stages of infection. Interestingly, expression of plastidic GS2, the major isoform of GS for Gln biosynthesis in leaves, was found to be downregulated during pathogen infection and senescence, which, in turn, causes a Gln deficiency in the chloroplast, a major site for Gln biosynthesis in normal plants. In this scenario, the Gln deficiency in chloroplasts in pathogen-infected wild-type tissues might be compensated for by importing cytosolic/apoplastic Gln via *LHT1* or upregulating the activities of spatially distinct cytosolic isoforms of GS1. Expression of GS1s was found to be upregulated upon pathogen infection, but the level of upregulation might not be as effective as *LHT1* in compensating for Gln content. Further investigation regarding the detailed relationship between GS1 and defenses is of great interest.

### Gln Homeostasis Modulates the Cellular Redox Status

Plant cells require a constant flux of energy for continuous biomass production and physiological functions, which can only

be achieved through cellular redox regulation when pools of ATP/ADP, NAD(P)H/NAD(P)<sup>+</sup>, and other redox carriers remain at balanced ratios.

The chloroplast, referred to as the powerhouse of photosynthetic cells, is also the major organelle involved in amino acid biosynthesis in plants. NH<sub>4</sub><sup>+</sup> is assimilated in the chloroplast by ATP-dependent amidation of the  $\gamma$ -carboxyl group of Glu by GS2 to form Gln. Subsequently, the amido group is transferred from Gln to 2-OG by Fd-GOGAT, with the concomitant consumption of reducing power (reduced ferredoxin) to form two molecules of Glu. One molecule reenters the GS/GOGAT cycle, and the other one represents the net product of NH<sub>4</sub><sup>+</sup> assimilation. Import of 2-OG and export of Glu across the chloroplast membrane are probably catalyzed by a two-translocator system consisting of a 2-OG/malate antiporter (DiT1) and a Glu/malate antiporter (DiT2) (Renné et al., 2003; Schneiderei et al., 2006). Thus, these malate shuttles would serve to export excess reducing equivalents from the chloroplast (Foyer et al., 2009).

When pathogens infect a plant, carbon fixation (Calvin cycle), the main sink for photosynthetic ATP and NADPH, and other primary metabolic pathways are downregulated. Photorespiration is another sink for electrons, particularly in C<sub>3</sub> plants subjected to high levels of light, high temperatures, low CO<sub>2</sub> concentrations, or water deficits, which ultimately facilitate redox exchange between intracellular compartments (Noctor, 2006; Foyer et al., 2009). Our microarray data indicate that transcripts for a set of photorespiration enzymes are largely repressed in *lht1*, as reported in the *Arabidopsis mpk4* mutant, which exhibits constitutive activation of SA-dependent defenses (Foyer et al., 2009). Therefore, a great challenge regarding pathogen-infected plant tissues will be how to protect them from photooxidation. Biosynthesis of Gln and Glu provides a strong electron sink, consuming both ATP and reducing power generated during photosynthesis (Baier and Dietz, 2005). We speculate that this role of Gln/Glu biosynthesis in consuming and translocating reducing equivalents becomes particularly important during pathogen infection: Gln deficiency in the plastid due to the inactivation of GS2 could inhibit the GS/GOGAT cycle. Therefore, maintaining GOGAT running smoothly in plastids by supplying Gln via LHT1 and/or cytosolic GS1 and the continuous malate valves would in part ensure the cellular redox balance and integrity during pathogen infection.

### Gln-Associated Redox Status Is Interconnected with the SA-Dependent Pathway

Our study shows that the *lht1*-conferred phenotypes are associated with the SA-dependant pathway. As discussed above, the deficiency of cytosolic Gln in *lht1* plants will hamper the translocation of reducing equivalents in the chloroplast and trigger a redox imbalance. Accumulation of ROS, such as H<sub>2</sub>O<sub>2</sub>, will eventually induce SA-dependent and light-modulated cell death (Dietrich et al., 1997; Mach et al., 2001; Genoud et al., 2002; Bechtold et al., 2005; Noctor, 2006), probably in part via the direct inactivation of the Gln-generating enzyme GS. Inactivation of GS by ROS or NO is indeed a very common phenomenon in both prokaryotic and eukaryotic cells (Ortega et al., 1999; Palatnik et al., 1999; Gómez-Baena et al., 2006). Notably,

*Arabidopsis* GS2 was the direct target of abundant redox-sensitive thioredoxins in chloroplasts (Motohashi et al., 2001).

The interconnections among Gln metabolism, redox, and SA contribute to our understanding of the SA-associated defense network. SA synthesized in chloroplasts is a crucial signaling molecule in defense responses, but little is known of its exact function in the defense signaling pathway. Growing evidence has demonstrated that the master SA pathway regulators, PAD4 and NPR1, act positively up- and downstream of SA, respectively, and are involved in or regulated by cellular redox status. PAD4, an undefined lipase-like protein, together with its signaling partner EDS1, plays central roles in modulating oxidative stress in chloroplasts and in promoting leaf senescence (Rustérucchi et al., 2001; Wiermer et al., 2005; Mateo et al., 2006; Ochsenbein et al., 2006; Mühlenbock et al., 2008). NPR1 encodes an I $\kappa$ B-like regulatory protein, and its activation is tightly regulated by an SA-induced redox change (Mou et al., 2003; Fobert and Després, 2005). More specifically, a recent study revealed that conformational changes (oligomer-monomer) of cytosolic NPR1 are regulated by the opposing actions of S-nitrosylation and TRX (Tada et al., 2008), in a mechanism reminiscent of GS2 modifications in chloroplasts, as discussed above. Our results provide further genetic evidence that Gln deficiency-induced ROS/NO accumulation might be the ultimate source of redox imbalance in both chloroplasts and the cytosol. These redox perturbations will suppress Gln biosynthesis via the inactivation of GS2 and further stimulate SA production, *PR* gene expression, and cell death via activation of PAD4 and NPR1. The SA-associated pathway might be one of the key executors that functions downstream of this redox relay.

In summary, we demonstrated an intriguing role of a developmentally important amino acid transporter LHT1 in plant-pathogen interactions. In our proposed model, LHT1 appears to operate as a master switch (safety valve) to coordinate the partition/allocation of Gln during the basal and systemic defense responses (Figure 9). During the progression of pathogen infection, the accumulation of electron equivalents driven by light predominantly in redox-active mesophyll cells is inevitable. The elevated reducing equivalents and subsequent ROS would inhibit GS2 and hence block Gln biosynthesis in chloroplasts. This in turn may augment the redox imbalance and promote the accumulation of ROS/SA in chloroplasts and subsequently in other compartments and eventually induce *PR* gene expression and cell death. To compensate for this deleterious effect, the affected host cells might be directed to acquire Gln, either from the biosynthesis via cytosolic GS1s or preferably from influx through the LHT1 transporter. Therefore, Gln homeostasis may be one of the checkpoints of life and death that is manipulated by both the host and the pathogen.

## METHODS

### Identification of *LHT1* Homologs

More than 50 amino acid transporters were reported in the *Arabidopsis thaliana* genome (Liu and Bush, 2006; Rentsch et al., 2007). Seven of them were closely related to LHT1, as determined by BLASTP ([www.Arabidopsis.org](http://www.Arabidopsis.org)), and analyzed by ClustalW using the conceptual translation products of cDNAs encoded by this gene family from the Arabidopsis Genome Annotation project. For simplicity, *LHT1*-like genes

maintained their previously described names (Bock et al., 2006) but included new members, *LHT9* and *LHT10*. *LHT2* expression has been reported to localize specifically to tapetum cells during seed development (Lee and Tegeder, 2004). Two previously assigned genes, *LHT4* and *LHT7*, were excluded from this cluster due to their low putative protein identities with *LHT1*, merely 37 and 32%, respectively.

#### Isolation of T-DNA Insertion Mutants and Generation of Double or Triple Mutants

All of the T-DNA insertion lines were generated by SIGnAL and obtained from the ABRC, except where specified. Six homozygous SALK lines (SALK\_034566, SALK\_036871, SALK\_026389, SALK\_115555, SALK\_000545, and SALK\_083700) that affect *LHT1* were screened by three rounds of PCR using both gene-specific and T-DNA left border primers (see Supplemental Table 2 online for oligo sequences used in this study). T-DNA insertions were confirmed by sequencing of the conjunction regions. Other T-DNA insertion lines that were identified by similar approaches and used in this study include *ald1-T2*, *apx1-T1*, *rbohD-T1*, *pad2-T1*, and *nudt7-T1*. The point mutation lines *npr1-3* (Cao et al., 1997), *sid2-1* (Nawrath and Métraux, 1999), *pad4-1* (Glazebrook et al., 1997), *ein2-1* (Roman et al., 1995), *etr1-1* (Chang et al., 1993), and *jar1-1* (Staswick et al., 2002), the transgene line *NahG* (Lawton et al., 1995), and the insertion/deletion line *nia1-1 nia2-5* (Wilkinson and Crawford, 1993) have been described elsewhere. All mutants were derived from the Columbia-0 (Col-0) background, except where noted. The double or triple mutants were generated by genetic crossings, and the homozygosity of these mutants was confirmed by PCR amplification, sequencing, and/or phenotypic screening when necessary. Detailed male/female parent pedigrees and their seed stock numbers are listed in Supplemental Table 1 online. All the oligo sequences used in this study for screening or DNA/cDNA amplification can be found in Supplemental Table 2 online.

#### Plant Growth, Pathogen Infection, and Disease Resistance Assays

*Arabidopsis* wild type (Col-0) and their corresponding mutants were grown routinely in growth chambers. Two illumination conditions, a 16-h photoperiod (long day) and an 8-h photoperiod (short day), were applied. The disease tests and gene expression analyses were performed at short-day conditions (Liu et al., 2005, 2007a).

*Pseudomonas syringae* pv *tomato* DC3000 strains harboring plasmid pVSP61 (virulent strain) or pV288 containing the *avrRpt2* gene (avirulent strain) (Maldonado et al., 2002) and a *hrcC* deletion mutant defective in protein secretion (Wei et al., 2000) were grown at 29°C in liquid King's B medium (Difco) containing rifampicin (100 µg mL<sup>-1</sup>) and kanamycin (50 µg mL<sup>-1</sup>). Overnight log phase cultures were grown to an optical density at OD<sub>600</sub> of ~0.6 to 0.8 (OD 0.1 = 10<sup>8</sup> colony-forming units (cfus) mL<sup>-1</sup>) and diluted with 10 mM MgCl<sub>2</sub> before inoculation. The bacterial suspensions were infiltrated into the abaxial surface of a leaf using a 1-mL syringe without a needle. The inoculation concentrations were 10<sup>5</sup> cfu mL<sup>-1</sup> for both virulent and avirulent strains and 10<sup>6</sup> cfu mL<sup>-1</sup> for the *hrcC* strain. Control inoculations were performed with 10 mM MgCl<sub>2</sub>. At various time points after inoculation, three sets of samples containing eight leaf disks (4 mm in diameter) randomly collected from several plants in each set were ground in 10 mM MgCl<sub>2</sub> and serially diluted. Each dilution was spread onto three to six plates containing King's B medium and antibiotics rifampicin (100 µg mL<sup>-1</sup>) and kanamycin (50 µg mL<sup>-1</sup>). Plates were incubated at 29°C for 2 d, and the number of colonies was recorded.

*Erysiphe cichoracearum* was maintained and propagated on cucumber (*Cucumis sativus*) plants (variety Sweet Slice, McKenzie, MB). Fresh mildewed cucumber plants were prepared every month. *Arabidopsis* plants were placed in settling towers and inoculated with conidia by

tapping heavily infected cucumber leaves above the *Arabidopsis* plants. High-density inoculations (20 to 50 conidia mm<sup>-2</sup>) were used for disease severity tests. Low-density inoculations (5 to 10 conidia mm<sup>-2</sup>) were employed for GS activity studies during the infection time course. After 30 min, the inoculated plants were returned to the growth chamber for further investigation.

*Colletotrichum higginsianum* Sacc, isolate (IMI349061), originating from *Brassica rapa*, was obtained from CAB International. The *C. higginsianum* was propagated and handled in experiments as described previously (Liu et al., 2007a). For disease assays, *Arabidopsis* plants were sprayed with conidial suspensions (1 × 10<sup>6</sup> spores mL<sup>-1</sup> in distilled water) or spotted with 12-µL droplets of the conidial suspension on the leaf surface on either side of the leaf midvein. Immediately after inoculation, the inoculated plants were placed in a 100% humidity chamber, where they remained for 2 d.

#### In Situ Detection of Reactive Oxygen/Nitrogen Species and Callose Accumulation

Macroscopic detection of H<sub>2</sub>O<sub>2</sub> accumulation by DAB staining was performed as described (Liu et al., 2007a, 2007b). Subcellular localization of H<sub>2</sub>O<sub>2</sub> and NO in pathogen-infected leaf tissues at various time points after inoculation were monitored by confocal laser scanning microscopy (Zeiss LSM510) after infiltration with 50 µM H<sub>2</sub>O<sub>2</sub>-sensitive dye, DCF-DA (Molecular Probes), or 10 µM NO-sensitive dye, DAF-DA (Molecular Probes), respectively, according to the dye-specific excitation/emission wavelength (488/505 to 530 nm for both dyes). Background chlorophyll autofluorescence emission was monitored with a 650-nm long-pass filter. Nuclear localization and the morphology of hypersensitively reacting cells were examined by dual staining with 10 µM Hoechst 33342 (Molecular Probes) and 10 µM propidium iodide (PI) under the excitation/emission wavelengths of 405/410 to 450 nm and 488/>560 nm, respectively, in multitrack mode.

For callose staining, whole leaves were collected at different time points after bacterial or fungal infection and stained with aniline blue (Hauck et al., 2003). Callose deposition was examined using an Axioplan epifluorescence microscope (Carl Zeiss).

#### Affymetrix ATH1 Array Analysis

*Arabidopsis* wild-type and *lht1-1* mutant plants were grown for 3 weeks in a short-day chamber, in the presence or absence of *Pst* DC3000 infiltration at a concentration of 10<sup>5</sup> cfu mL<sup>-1</sup>. Total RNA was extracted using the phenol/chloroform/LiCl method from leaves 48 h after pathogen infection. Homogeneous populations of leaves were used to better represent expression profiles. To that end, leaves at the same stages (fully expanded) were hand-selected and pooled together for each biological replicate. Biotinylated cRNA was prepared according to the standard Affymetrix protocol from 6 to 10 µg total RNA. Hybridization, washing, and scanning were performed at the Bio-Array Resource Center, University of Toronto, using *Arabidopsis* ATH1 genome oligonucleotide chips ([www.csb.utoronto.ca/resources/facilities/affymetrix-genechip](http://www.csb.utoronto.ca/resources/facilities/affymetrix-genechip)). The reproducibility of the microarray analysis was assayed by triplicate replication of each experiment. For analysis, 12 microarrays were imported into R package Affy (Gautier et al., 2004). Subsequent background correction and quantile normalization were performed with all microarrays using the robust multianalysis package implemented in Bioconductor (<http://www.bioconductor.org>). Model-based analysis was performed by perfect match only analysis using the R package linear model of microarray analysis (LIMMA) (Smyth, 2004). By reading the data and creating an expression set of the data after log<sub>2</sub> transformation, a linear model was fitted and pairwise comparisons were performed. The LIMMA package was used because it has better precision than Microarray Suite version 5.0 (MAS 5.0) and it is suitable for experiments with

a small sample size (Bolstad et al., 2003). For each probe, a fold change and corresponding P value measuring the statistical significance of differentially expressed genes were calculated from an empirical Bayes approach to compute moderated t-statistics (Smyth, 2004). All of the P values were then corrected for multiple testing by applying false discovery rate from Benjamini and Hochberg (1995). Genes were considered differentially expressed if the P value was <0.05 and the fold change in expression level was >2. An overall test of significance for a gene that is differentially expressed on any contrast was prepared in LIMMA. Venn diagrams were generated from two contrasts to examine the overlapping genes using F-statistics with a P value below 0.05 (Smyth, 2004). Gene functional annotations were obtained from the Bio-Array Resource Center using the probe set numbers provided by the GeneChip manufacturer (Affymetrix). Biochemical pathway analyses were conducted using the AraCyc database ([www.Arabidopsis.org/tools/araCyc](http://www.Arabidopsis.org/tools/araCyc)).

### Profiling of Amino Acids

Three sets of pooled leaves were collected from wild-type or mutant plants 3, 6, and 9 DAI with *Ec*. Materials were collected at the same time points for control wild-type and mutant plants. The samples were extracted using the EZ:faast Kit (Phenomenex). Amino acids were separated by gas chromatography–mass spectrometry (Pickering Laboratories), and data were analyzed according to the manufacturer's instructions.

### Generation of Promoter-GUS Fusions and Transgenic Plants

The promoter-GUS fusion consisted of the region 1906-bp upstream of the *LHT1* start codon promoter and *uidA* (GUS). The promoter fragments were amplified from genomic DNA using primers 5'-GTCGACGA-ATTCTCCATAGACGAGTACGAGAGA-3' and 5'-CCATGGATCCGGT-GAGAGGTTGAGAGGGAGA-3', which incorporated flanking restriction enzyme sites *RcoRI* and *NcoI*, respectively. The fragment was then subcloned into *EcoRI/NcoI* in pBluescript SK (Stratagene). After verifying the sequence fidelity by sequencing, the promoter was fused into the same restriction sites in frame with *uidA* of pCambia3301 to replace the constitutive promoter cauliflower mosaic virus 35S. The fusion construct was transformed into *Agrobacterium tumefaciens* strain EHA105 by electroporation and subsequently into *Arabidopsis* using the floral dip method described by Clough and Bent (1998). The GUS staining patterns of transgenic plants were examined before and after pathogen infections as described (Jefferson et al., 1987).

### GFP Detection in Transgenic Plants Using Confocal Microscopy

Transgenic *AMT1;1<sub>pro</sub>-AMT1;1-GFP Arabidopsis* leaves were subjected to confocal microscopy to detect GFP fluorescence (green) at 3 DAI with *Ec*. The red fluorescence of PI (5 ng mL<sup>-1</sup>) was used to visualize plant cell walls and fungal haustoria.

### Seedling Plate Assays

To examine seedling growth on plates, surface-sterilized seeds were planted on complete MS medium or MS without a nitrogen source (MS-N) and supplemented with different concentrations of amino acids or other chemicals, based on the experimental design. The chemicals were purchased from Sigma-Aldrich or Alfa Aesar, and all the media were supplemented with 2% sucrose and 1% Bacto agar (BD Bioscience). All supplemental compounds were filter sterilized before being added to the base medium.

### Plant Treatment with Chemicals

For the analysis of reactive oxygen/nitrogen species on GS activity, the 4-week-old *Arabidopsis* wild-type leaves were infiltrated with solutions

containing 0.5 mM glucose and 0.5 units mL<sup>-1</sup> of glucose oxidase (which produces a sustained level of 6 to 10 μM of H<sub>2</sub>O<sub>2</sub> in plant cells; Delledonne et al., 1998), with or without the addition of 300 units mL<sup>-1</sup> catalase, 0.5 mM sodium nitroprusside (a NO donor equivalent to 1.2 μM NO in plant cells; Delledonne et al., 2001), with or without the addition of 500 μM 2-(4-carboxyphenyl)-4,4,5,5-tetramethyl-imidazole-1-oxyl-3-oxide (a NO scavenger), or with or without the addition of both glucose oxidase and sodium nitroprusside. The leaves were collected at 3, 8, and 12 h after treatments for protein extraction and the GS activity assay.

To determine the effect of L-PPT treatment on chlorosis development and defense gene expression, 4-week-old plants were sprayed with different concentrations of L-PPT. The treated leaves were photographed at a time course or collected for further analyses (e.g., RNA gel blotting). To establish the effect of Gln on H<sub>2</sub>O<sub>2</sub> production, the leaves were stained with DAB 24 h after infiltration with various concentrations of Gln. To gauge the effect of Gln on L-PPT-induced cell death, the leaves were sprayed with 10 μg mL<sup>-1</sup> of L-PPT immediately after infiltration with 0.1, 1, or 10 mg mL<sup>-1</sup> of Gln.

### Measurement of Free SA

Four-week-old plants were sprayed with 10<sup>7</sup> cfu mL<sup>-1</sup> of *Pst* DC3000 suspension containing 0.02% Silwet L-77 (Lehle Seeds) or inoculated with 10<sup>6</sup> mL<sup>-1</sup> of *Ch* conidia and then incubated under 100% humidity in a growth chamber (18 ± 2°C with an 8-h photoperiod at a light intensity of 150 μE m<sup>-2</sup> s<sup>-1</sup>). Mock-treated plants were employed as controls. One hundred grams of ground tissue was extracted and analyzed by HPLC–mass spectrometry at the indicated times (Quattro Ultima; Micromass) according to a previously published protocol (Chiwocha et al., 2003).

### RNA Gel Blot Analyses

*Arabidopsis* leaves, inoculated or not, were collected at various intervals as specified, flash frozen in liquid nitrogen, and stored at –80°C until required. Total RNA extraction from control or treated leaves as well as RNA gel blot analysis was performed as described (Liu et al., 2005). Probes, consisting of the entire or partial coding region of *LHT1*, seven *LHT1*-like genes, *PR1*, *PR2*, *PDF1.2*, and *AMT1;1* were amplified by either RT-PCR using gene-specific primer pairs, at least one of which was specific for 5'- or 3'-untranslated regions, or by PCR from cloned plasmids. The RT-PCR was performed using total mRNAs that were isolated from whole plants of wild-type *Arabidopsis*. The RT-PCR products were visualized in agarose gels using ethidium bromide staining, purified using a QIAquick PCR purification kit (Qiagen), and confirmed by sequencing. The introduction of 5'- or 3'-untranslated regions during primer design improves efficiency and specificity for both amplification and hybridization. The oligo sequences of these primers are listed in Supplemental Table 2 online. All RNA gel blot analyses were conducted with at least two biological replicates.

### Chloroplast Isolation

High-efficiency chloroplast isolations were performed according to Rensink et al. (1998) from 4-week-old *Arabidopsis* wild-type rosette leaves 3 to 6 DAI with *Ec* or a mock inoculation. Briefly, 10 g fresh weight of leaves were collected and ground in a polytron blender in 100 mL of ice-cold buffer (330 mM sorbitol, 20 mM tricine/KOH, pH 8.4, 5 mM EGTA, 5 mM EDTA, 10 mM NaCO<sub>3</sub>, 0.1% BSA, and 330 mg L<sup>-1</sup> ascorbate). The suspension was filtered and centrifuged for 5 min at 3000 rpm to harvest the crude chloroplast fraction. The crude fraction was resuspended in 40% (v/v) Percoll/grinding buffer and topped onto 10 mL of Percoll/grinding buffer gradient consisting of 2 mL of 70% (v/v) (bottom), 4 mL of 50% (v/v) (middle), and 4 mL of 40% (v/v) (top), respectively, in a 15-mL polycarbonate tube, then followed by centrifugation for 15 min at 5000

rpm in a HB-4 rotor with the brake off. The interface between 50% and 70% Percoll/grinding buffer was harvested. The chloroplasts were isolated by centrifugation and resuspended in 3 volumes of grinding buffer. The intactness of the chloroplasts was assessed by microscopy and found to be >85%. Chloroplast suspensions were directly used for protein extraction or stored at  $-80^{\circ}\text{C}$  for further use.

#### Protein Extraction and Immunoblot and Enzyme Activity Assays

The protocols used for protein extraction and immunoblot analysis were as described by Bennett and Cullimore (1989), with some modifications. Briefly, *Arabidopsis* leaves were ground in liquid nitrogen and homogenized in a solution (50 mM Tris, pH 8.0, 2 mM EDTA, 10% [v/v] glycerol, and 10 mM 2-mercaptoethanol). The homogenates were centrifuged at 12,000 rpm for 3 min at  $4^{\circ}\text{C}$ . Total protein concentration was determined using the Bradford assay (Bradford, 1976), with BSA as standard. About 8  $\mu\text{g}$  of protein was separated by 12% SDS-PAGE, electroblotted onto polyvinylidene fluoride membrane (Bio-Rad), and blocked with TTBS (20 mM Tris, pH 7.6, 137 mM NaCl, and 0.1% [v/v] Tween 20) containing 4% skim milk. The blocked blot was then incubated with 18  $\mu\text{g}$  of lyophilized anti-GS serum (Bennett and Cullimore, 1989) in 10 mL of TTBS at  $37^{\circ}\text{C}$  for 2 h. After several washes with TTBS, the membrane was incubated at room temperature for 2 h with horseradish peroxidase-conjugated anti-rabbit IgG (1:15,000) (Amersham), and the immune complexes were detected using enhanced chemifluorescence reagents.

The activity of Gln synthetase was measured following a modified procedure of Bennett and Cullimore (1989). Isolated proteins were preincubated in GS activity assay buffer (70 mM MOPS, pH 6.8, 100 mM Glu, 50 mM  $\text{MgSO}_4$ , 15 mM  $\text{NH}_2\text{OH}$ , and 15 mM ATP) at  $37^{\circ}\text{C}$  for 30 min. The reaction was then terminated by adding an acidic  $\text{FeCl}_3$  solution, consisting of 88 mM  $\text{FeCl}_3$ , 670 mM HCl, and 200 mM trichloroacetic acid. The products were quantified spectrophotometrically at 498 nm using  $\gamma$ -glutamyl hydroxymate as the standard.

#### Accession Numbers

Sequence data from this article can be found in the Arabidopsis Genome Initiative or GenBank/EMBL databases under the following accession numbers: *PR1* (At2g14610), *PR2* (At3g57260), *PDF1.2* (At5g44420), *AMT1;1* (At4g13510), *LHT1* (At5g40780), *LHT2* (At1g24400), *LHT3* (At1g61270), *LHT4* (At1g47670), *LHT5* (At1g67640), *LHT6* (At3g01760), *LHT7* (At4g35180), *LHT8* (At1g71680), *LHT9* (At1g48640), *LHT10* (At1g25530), *NPR1* (At1g64280), *PAD4* (At3g52430), *SID2* (At1g74710), *JAR1* (At2g46370), *EIN2* (At5g03280), *ETR1* (At1g66340), *APX1* (At1g07890), *RBOHD* (At5g47910), *ALD1* (At2g13810), *NUDT7* (At4g12720), *NIA1* (At1g77760), *NIA2* (At1g37130), and *GDU1* (At4g31730). The microarray data are accessible under accession number GSE19109 (<http://www.ncbi.nlm.nih.gov/geo/query/acc.cgi?acc=GSE19109>).

#### Supplemental Data

The following materials are available in the online version of this article.

**Supplemental Figure 1.** Characterization of *LHT1* T-DNA Mutations.

**Supplemental Figure 2.** Enhanced Defense Responses in *LHT1* in Response to Pathogen Attack.

**Supplemental Figure 3.** Constitutive Localization of *LHT1*<sub>pro</sub>-GUS Activity.

**Supplemental Figure 4.** Expressions of Genes Homologous to *LHT1*.

**Supplemental Figure 5.** Expression of *LHT1* in Defense Pathway-Impaired Mutants.

**Supplemental Figure 6.** Developmental Phenotypes of *LHT1* Knock-out under Different Light Conditions.

**Supplemental Figure 7.** Enhanced NO Accumulation in the Nuclei of *lht1* Mutant after Pathogen Infection.

**Supplemental Figure 8.** Differentially Expressed Genes in *lht1* Mutant and in Pathogen-Challenged Wild-Type Plants.

**Supplemental Figure 9.** The Sensitivity of Wild-Type and *lht1* Seedlings to D-Amino Acids.

**Supplemental Figure 10.** Gln Suppresses  $\text{H}_2\text{O}_2$  Accumulation and L-PPT-Induced Leaf Chlorosis.

**Supplemental Figure 11.** Phenotype of *lht1 gdu1* Double Mutant Plants.

**Supplemental Table 1.** Double or Triple Mutants Generated by Genetic Crossing in This Study.

**Supplemental Table 2.** Primers Used in This Study.

**Supplemental Data Set 1.** The Sequences and Alignment of LHT1-Like Proteins Used for Generating the Phylogenetic Tree.

#### ACKNOWLEDGMENTS

We thank Vipen Sawhney for critical reading of the manuscript and John Li for assistance of microarray analysis. We thank Julie Cullimore for providing GS antiserum, Uwe Ludewig for AMT1;1-GFP seeds, and Shen-Yang He for *Pst hrcC* strain. Other *Arabidopsis* seeds were obtained from the ABRC (Ohio State University). This work was supported by a Natural Sciences and Engineering Research Council of Canada grant to Y.W.

Received September 13, 2010; revised September 13, 2010; accepted October 28, 2010; published November 19, 2010.

#### REFERENCES

- Ahn, I.P. (2008). Glufosinate ammonium-induced pathogen inhibition and defense responses culminate in disease protection in bar-transgenic rice. *Plant Physiol.* **146**: 213–227.
- Baier, M., and Dietz, K.J. (2005). Chloroplasts as source and target of cellular redox regulation: A discussion on chloroplast redox signals in the context of plant physiology. *J. Exp. Bot.* **56**: 1449–1462.
- Bartsch, M., Gobatto, E., Bednarek, P., Debey, S., Schultze, J.L., Bautor, J., and Parker, J.E. (2006). Salicylic acid-independent ENHANCED DISEASE SUSCEPTIBILITY1 signaling in *Arabidopsis* immunity and cell death is regulated by the monooxygenase FMO1 and the Nudix hydrolase NUDT7. *Plant Cell* **18**: 1038–1051.
- Bechtold, U., Karpinski, S., and Mullineaux, P.M. (2005). The influence of the light environment and photosynthesis on oxidative signaling responses in plant-biotrophic pathogen interactions. *Plant Cell Environ.* **28**: 1046–1055.
- Benjamini, Y., and Hochberg, Y. (1995). Controlling the false discovery rate: a practical and powerful approach to multiple testing. *J. R. Stat. Soc.* **57**: 289–300.
- Bennett, M.J., and Cullimore, J.V. (1989). Glutamine synthetase isoenzymes of *Phaseolus vulgaris* L.: Subunits composition in developing root nodules and plumules. *Planta* **179**: 433–440.
- Berger, S., Sinha, A.K., and Roitsch, T. (2007). Plant physiology meets phytopathology: plant primary metabolism and plant-pathogen interactions. *J. Exp. Bot.* **58**: 4019–4026.
- Blume, M., Rodriguez-Contreras, D., Landfear, S., Fleige, T., Soldati-Favre, D., Lucius, R., and Gupta, N. (2009). Host-derived



- glucose and its transporter in the obligate intracellular pathogen *Toxoplasma gondii* are dispensable by glutaminolysis. *Proc. Natl. Acad. Sci. USA* **106**: 12998–13003.
- Bock, K.W., Honys, D., Ward, J.M., Padmanaban, S., Nawrocki, E.P., Hirschi, K.D., Twell, D., and Sze, H.** (2006). Integrating membrane transport with male gametophyte development and function through transcriptomics. *Plant Physiol.* **140**: 1151–1168.
- Bolstad, B.M., Irizarry, R.A., Astrand, M., and Speed, T.P.** (2003). A comparison of normalization methods for high density oligonucleotide array data based on variance and bias. *Bioinformatics* **19**: 185–193.
- Bradford, M.M.** (1976). A rapid and sensitive method for the quantitation of microgram quantities of protein utilizing the principle of protein-dye binding. *Anal. Biochem.* **72**: 248–254.
- Cao, H., Glazebrook, J., Clarke, J.D., Volko, S., and Dong, X.** (1997). The Arabidopsis NPR1 gene that controls systemic acquired resistance encodes a novel protein containing ankyrin repeats. *Cell* **88**: 57–63.
- Chang, C., Kwok, S.F., Bleeker, A.B., and Meyerowitz, E.M.** (1993). Arabidopsis ethylene-response gene ETR1: similarity of product to two-component regulators. *Science* **262**: 539–544.
- Chen, L., and Bush, D.R.** (1997). LHT1, a lysine- and histidine-specific amino acid transporter in Arabidopsis. *Plant Physiol.* **115**: 1127–1134.
- Chiwocha, S.D., Abrams, S.R., Ambrose, S.J., Cutler, A.J., Loewen, M., Ross, A.R., and Kermode, A.R.** (2003). A method for profiling classes of plant hormones and their metabolites using liquid chromatography-electrospray ionization tandem mass spectrometry: An analysis of hormone regulation of thermodormancy of lettuce (*Lactuca sativa* L.) seeds. *Plant J.* **35**: 405–417.
- Clough, S.J., and Bent, A.F.** (1998). Floral dip: A simplified method for Agrobacterium-mediated transformation of *Arabidopsis thaliana*. *Plant J.* **16**: 735–743.
- Coruzzi, G.M.** (September 30, 2003). Primary N-assimilation into amino acids in *Arabidopsis*. In *The Arabidopsis Book*, C.R. Somerville and E.M. Meyerowitz, eds (Rockville, MD: American Society of Plant Biologists), doi/10.1199/tab.0010, <http://www.aspb.org/publications/arabidopsis/>.
- Davletova, S., Rizhsky, L., Liang, H., Shengqiang, Z., Oliver, D.J., Coutu, J., Shulaev, V., Schlauch, K., and Mittler, R.** (2005). Cytosolic ascorbate peroxidase 1 is a central component of the reactive oxygen gene network of *Arabidopsis*. *Plant Cell* **17**: 268–281.
- Delledonne, M., Xia, Y., Dixon, R.A., and Lamb, C.** (1998). Nitric oxide functions as a signal in plant disease resistance. *Nature* **394**: 585–588.
- Delledonne, M., Zeier, J., Marocco, A., and Lamb, C.** (2001). Signal interactions between nitric oxide and reactive oxygen intermediates in the plant hypersensitive disease resistance response. *Proc. Natl. Acad. Sci. USA* **98**: 13454–13459.
- Dietrich, R.A., Richberg, M.H., Schmidt, R., Dean, C., and Dangi, J.L.** (1997). A novel zinc finger protein is encoded by the *Arabidopsis* LSD1 gene and functions as a negative regulator of plant cell death. *Cell* **88**: 685–694.
- Divon, H.H., and Fluhr, R.** (2007). Nutrition acquisition strategies during fungal infection of plants. *FEMS Microbiol. Lett.* **266**: 65–74.
- Dong, X.N.** (2004). NPR1, all things considered. *Curr. Opin. Plant Biol.* **7**: 547–552.
- Erikson, O., Hertzberg, M., and Näsholm, T.** (2004). A conditional marker gene allowing both positive and negative selection in plants. *Nat. Biotechnol.* **22**: 455–458.
- Feller, U., Anders, I., and Mae, T.** (2008). Rubiscolytics: Fate of Rubisco after its enzymatic function in a cell is terminated. *J. Exp. Bot.* **59**: 1615–1624.
- Fischer, W.N., Andre, B., Rentsch, D., Krolkiewicz, S., Tegeder, M., Breitzkreuz, K., and Frommer, W.B.** (1998). Amino acid transport in plants. *Trends Plant Sci.* **3**: 188–195.
- Fobert, P.R., and Després, C.** (2005). Redox control of systemic acquired resistance. *Curr. Opin. Plant Biol.* **8**: 378–382.
- Forsum, O., Svennerstam, H., Ganeteg, U., and Näsholm, T.** (2008). Capacities and constraints of amino acid utilization in *Arabidopsis*. *New Phytol.* **179**: 1058–1069.
- Foyer, C.H., Bloom, A.J., Queval, G., and Noctor, G.** (2009). Photorespiratory metabolism: genes, mutants, energetics, and redox signaling. *Annu. Rev. Plant Biol.* **60**: 455–484.
- Foyer, C.H., and Noctor, G.** (2005). Redox homeostasis and antioxidant signaling: a metabolic interface between stress perception and physiological responses. *Plant Cell* **17**: 1866–1875.
- Gautier, L., Cope, L.M., Bolstad, B.M., and Irizarry, R.A.** (2004). affy—analysis of Affymetrix GeneChip data at the probe level. *Bioinformatics* **20**: 307–315.
- Ge, X., Li, G.J., Wang, S.B., Zhu, H., Zhu, T., Wang, X., and Xia, Y.** (2007). AtNUDT7, a negative regulator of basal immunity in Arabidopsis, modulates two distinct defense response pathways and is involved in maintaining redox homeostasis. *Plant Physiol.* **145**: 204–215.
- Genoud, T., Buchala, A.J., Chua, N.H., and Métraux, J.P.** (2002). Phytochrome signalling modulates the SA-perceptive pathway in *Arabidopsis*. *Plant J.* **31**: 87–95.
- Glazebrook, J., Zook, M., Mert, F., Kagan, I., Rogers, E.E., Crute, I. R., Holub, E.B., Hammerschmidt, R., and Ausubel, F.M.** (1997). Phytoalexin-deficient mutants of Arabidopsis reveal that PAD4 encodes a regulatory factor and that four PAD genes contribute to downy mildew resistance. *Genetics* **146**: 381–392.
- Gómez-Baena, G., Manuel García-Fernández, J., López-Lozano, A., Toribio, F., and Diez, J.** (2006). Glutamine synthetase degradation is controlled by oxidative proteolysis in the marine cyanobacterium *Prochlorococcus marinus* strain PCC 9511. *Biochim. Biophys. Acta* **1760**: 930–940.
- Hahn, M., Neef, U., Struck, C., Göttfert, M., and Mendgen, K.** (1997). A putative amino acid transporter is specifically expressed in haustoria of the rust fungus *Uromyces fabae*. *Mol. Plant Microbe Interact.* **10**: 438–445.
- Ham, J.H., Kim, M.G., Lee, S.Y., and Mackey, D.** (2007). Layered basal defenses underlie non-host resistance of *Arabidopsis* to *Pseudomonas syringae* pv. *phaseolicola*. *Plant J.* **51**: 604–616.
- Hauck, P., Thilmony, R., and He, S.Y.** (2003). A *Pseudomonas syringae* type III effector suppresses cell wall-based extracellular defense in susceptible *Arabidopsis* plants. *Proc. Natl. Acad. Sci. USA* **100**: 8577–8582.
- Hirner, A., Ladwig, F., Stransky, H., Okumoto, S., Keinath, M., Harms, A., Frommer, W.B., and Koch, W.** (2006). *Arabidopsis* LHT1 is a high-affinity transporter for cellular amino acid uptake in both root epidermis and leaf mesophyll. *Plant Cell* **18**: 1931–1946.
- Hofreuter, D., Novik, V., and Galán, J.E.** (2008). Metabolic diversity in *Campylobacter jejuni* enhances specific tissue colonization. *Cell Host Microbe* **4**: 425–433.
- Jefferson, R.A., Kavanagh, T.A., and Bevan, M.W.** (1987). GUS fusions:  $\beta$ -Glucuronidase as a sensitive and versatile gene fusion marker in higher plants. *EMBO J.* **6**: 3901–3907.
- Jones, J.D., and Dangi, J.L.** (2006). The plant immune system. *Nature* **444**: 323–329.
- Lawton, K.A., Weymann, K., Friedrich, L., Vernooij, B., Uknes, S., and Ryals, J.** (1995). Systemic acquired resistance in Arabidopsis requires salicylic acid but not ethylene. *Mol. Plant Microbe Interact.* **8**: 863–870.
- Lee, Y.H., and Tegeder, M.** (2004). Selective expression of a novel high-affinity transport system for acidic and neutral amino acids in the tapetum cells of *Arabidopsis* flowers. *Plant J.* **40**: 60–74.
- Liu, G., Greenshields, D.L., Sammynaiken, R., Hirji, R.N., Selvaraj, G., and Wei, Y.** (2007b). Targeted alterations in iron homeostasis underlie plant defense responses. *J. Cell Sci.* **120**: 596–605.
- Liu, G., Holub, E.B., Alonso, J.M., Ecker, J.R., and Fobert, P.R.**

- (2005). An *Arabidopsis* NPR1-like gene, NPR4, is required for disease resistance. *Plant J.* **41**: 304–318.
- Liu, G., Kennedy, R., Greenshields, D.L., Peng, G., Forseille, L., Selvaraj, G., and Wei, Y.** (2007a). Detached and attached *Arabidopsis* leaf assays reveal distinctive defense responses against hemibiotrophic *Colletotrichum* spp. *Mol. Plant Microbe Interact.* **20**: 1308–1319.
- Liu, X., and Bush, D.R.** (2006). Expression and transcriptional regulation of amino acid transporters in plants. *Amino Acids* **30**: 113–120.
- Mach, J.M., Castillo, A.R., Hoogstraten, R., and Greenberg, J.T.** (2001). The *Arabidopsis*-accelerated cell death gene ACD2 encodes red chlorophyll catabolite reductase and suppresses the spread of disease symptoms. *Proc. Natl. Acad. Sci. USA* **98**: 771–776.
- Maldonado, A.M., Doerner, P., Dixon, R.A., Lamb, C.J., and Cameron, R.K.** (2002). A putative lipid transfer protein involved in systemic resistance signalling in *Arabidopsis*. *Nature* **419**: 399–403.
- Martínez, D.E., Costa, M.L., Gomez, F.M., Otegui, M.S., and Guamet, J.J.** (2008). ‘Senescence-associated vacuoles’ are involved in the degradation of chloroplast proteins in tobacco leaves. *Plant J.* **56**: 196–206.
- Mateo, A., Funck, D., Mühlenbock, P., Kular, B., Mullineaux, P.M., and Karpinski, S.** (2006). Controlled levels of salicylic acid are required for optimal photosynthesis and redox homeostasis. *J. Exp. Bot.* **57**: 1795–1807.
- Mittler, R., Vanderauwera, S., Gollery, M., and Van Breusegem, F.** (2004). Reactive oxygen gene network of plants. *Trends Plant Sci.* **9**: 490–498.
- Motohashi, K., Kondoh, A., Stumpp, M.T., and Hisabori, T.** (2001). Comprehensive survey of proteins targeted by chloroplast thioredoxin. *Proc. Natl. Acad. Sci. USA* **98**: 11224–11229.
- Mou, Z., Fan, W.H., and Dong, X.N.** (2003). Inducers of plant systemic acquired resistance regulate NPR1 function through redox changes. *Cell* **113**: 935–944.
- Mühlenbock, P., Szechynska-Hebda, M., Plaszczycza, M., Baudo, M., Mateo, A., Mullineaux, P.M., Parker, J.E., Karpinska, B., and Karpinski, S.** (2008). Chloroplast signaling and LESION SIMULATING DISEASE1 regulate crosstalk between light acclimation and immunity in *Arabidopsis*. *Plant Cell* **20**: 2339–2356. Erratum. *Plant Cell* **20**: 3480.
- Nawrath, C., and Métraux, J.-P.** (1999). Salicylic acid induction-deficient mutants of *Arabidopsis* express PR-2 and PR-5 and accumulate high levels of camalexin after pathogen inoculation. *Plant Cell* **11**: 1393–1404.
- Navarro, L., Bari, R., Achard, P., Lisón, P., Nemri, A., Harberd, N.P., and Jones, J.D.** (2008). DELLAs control plant immune responses by modulating the balance of jasmonic acid and salicylic acid signaling. *Curr. Biol.* **18**: 650–655.
- Noctor, G.** (2006). Metabolic signalling in defence and stress: The central roles of soluble redox couples. *Plant Cell Environ.* **29**: 409–425.
- Ochsenbein, C., Przybyla, D., Danon, A., Landgraf, F., Göbel, C., Imboden, A., Feussner, I., and Apel, K.** (2006). The role of EDS1 (enhanced disease susceptibility) during singlet oxygen-mediated stress responses of *Arabidopsis*. *Plant J.* **47**: 445–456.
- Ortega, J.L., Roche, D., and Sengupta-Gopalan, C.** (1999). Oxidative turnover of soybean root glutamine synthetase. In vitro and in vivo studies. *Plant Physiol.* **119**: 1483–1496.
- Pageau, K., Reisdorf-Cren, M., Morot-Gaudry, J.F., and Masclaux-Daubresse, C.** (2006). The two senescence-related markers, GS1 and GDH, involved in nitrogen mobilization, are differentially regulated during pathogen attack and by stress hormones and reactive oxygen species in *Nicotiana tabacum* L. leaves. *J. Exp. Bot.* **57**: 547–557.
- Palatnik, J.F., Carrillo, N., and Valle, E.M.** (1999). The role of photosynthetic electron transport in the oxidative degradation of chloroplast glutamine synthetase. *Plant Physiol.* **121**: 471–478.
- Parisy, V., Poinssot, B., Owsianowski, L., Buchala, A., Glazebrook, J., and Mauch, F.** (2007). Identification of PAD2 as a gamma-glutamylcysteine synthetase highlights the importance of glutathione in disease resistance of *Arabidopsis*. *Plant J.* **49**: 159–172.
- Pellier, A.L., Laugé, R., Veneault-Fourrey, C., and Langin, T.** (2003). CLNR1, the AREA/NIT2-like global nitrogen regulator of the plant fungal pathogen *Colletotrichum lindemuthianum* is required for the infection cycle. *Mol. Microbiol.* **48**: 639–655.
- Perez-Garcia, A., Canovas, F.M., Gallardo, F., Hirel, B., and Devicente, A.** (1995). Differential expression of glutamine-synthetase isoforms in tomato detached leaflets infected with *Pseudomonas syringae* pv tomato. *Mol. Plant Microbe Interact.* **8**: 96–103.
- Perez-Garcia, A., Pereira, S., Pissarra, J., Gutierrez, A.G., Cazoria, F.M., Salema, R., de Vicente, A., and Canovas, F.M.** (1998). Cytosolic localization in tomato mesophyll cells of a novel glutamine synthetase induced in response to bacterial infection or phosphinothricin treatment. *Planta* **206**: 426–434.
- Pilot, G., Stransky, H., Bushey, D.F., Pratelli, R., Ludewig, U., Wingate, V.P.M., and Frommer, W.B.** (2004). Overexpression of GLUTAMINE DUMPER1 leads to hypersecretion of glutamine from hydathodes of *Arabidopsis* leaves. *Plant Cell* **16**: 1827–1840.
- Rawat, S.R., Silim, S.N., Kronzucker, H.J., Siddiqi, M.Y., and Glass, A.D.** (1999). AtAMT1 gene expression and NH<sub>4</sub><sup>+</sup> uptake in roots of *Arabidopsis thaliana*: Evidence for regulation by root glutamine levels. *Plant J.* **19**: 143–152.
- Renné, P., Dressen, U., Hebbeker, U., Hille, D., Flügge, U.I., Westhoff, P., and Weber, A.P.** (2003). The *Arabidopsis* mutant dct is deficient in the plastidic glutamate/malate translocator DIT2. *Plant J.* **35**: 316–331.
- Rensink, W.A., Pilon, M., and Weisbeek, P.** (1998). Domains of a transit sequence required for in vivo import in *Arabidopsis* chloroplasts. *Plant Physiol.* **118**: 691–699.
- Rentsch, D., Schmidt, S., and Tegeder, M.** (2007). Transporters for uptake and allocation of organic nitrogen compounds in plants. *FEBS Lett.* **581**: 2281–2289.
- Roman, G., Lubarsky, B., Kieber, J.J., Rothenberg, M., and Ecker, J.R.** (1995). Genetic analysis of ethylene signal transduction in *Arabidopsis thaliana*: Five novel mutant loci integrated into a stress response pathway. *Genetics* **139**: 1393–1409.
- Rustérucci, C., Aviv, D.H., Holt III, B.F., Dangl, J.L., and Parker, J.E.** (2001). The disease resistance signaling components EDS1 and PAD4 are essential regulators of the cell death pathway controlled by LSD1 in *Arabidopsis*. *Plant Cell* **13**: 2211–2224.
- Shah, J.** (2003). The salicylic acid loop in plant defense. *Curr. Opin. Plant Biol.* **6**: 365–371.
- Schneidereit, J., Häusler, R.E., Fiene, G., Kaiser, W.M., and Weber, A.P.** (2006). Antisense repression reveals a crucial role of the plastidic 2-oxoglutarate/malate translocator DIT1 at the interface between carbon and nitrogen metabolism. *Plant J.* **45**: 206–224.
- Smyth, G.K.** (2004). Linear models and empirical bayes methods for assessing differential expression in microarray experiments. *Stat. Appl. Genet. Mol. Biol.* **3**: Article 3.
- Snoeijs, S.S., Perez-Garcia, A., Joosten, M.H.A.J., and De Wit, P.J.G.M.** (2000). The effect of nitrogen on disease development and gene expression in bacterial and fungal plant pathogens. *Eur. J. Plant Pathol.* **106**: 493–506.
- Solomon, P.S., Tan, K.C., and Oliver, R.P.** (2003). The nutrient supply of pathogenic fungi: a fertile field for study. *Mol. Plant Pathol.* **4**: 203–210.
- Song, J.T., Lu, H., McDowell, J.M., and Greenberg, J.T.** (2004). A key role for ALD1 in activation of local and systemic defenses in *Arabidopsis*. *Plant J.* **40**: 200–212.
- Spanu, P., and Kämper, J.** (2010). Genomics of biotrophy in fungi and oomycetes—Emerging patterns. *Curr. Opin. Plant Biol.* **13**: 409–414.
- Spoel, S.H., Johnson, J.S., and Dong, X.** (2007). Regulation of trade-offs between plant defenses against pathogens with different lifestyles. *Proc. Natl. Acad. Sci. USA* **104**: 18842–18847.

- Staswick, P.E., Tiryaki, I., and Rowe, M.L.** (2002). Jasmonate response locus JAR1 and several related *Arabidopsis* genes encode enzymes of the firefly luciferase superfamily that show activity on jasmonic, salicylic, and indole-3-acetic acids in an assay for adenylation. *Plant Cell* **14**: 1405–1415.
- Svennerstam, H., Ganeteg, U., Bellini, C., and Näsholm, T.** (2007). Comprehensive screening of *Arabidopsis* mutants suggests the lysine histidine transporter 1 to be involved in plant uptake of amino acids. *Plant Physiol.* **143**: 1853–1860.
- Tada, Y., Spoel, S.H., Pajerowska-Mukhtar, K., Mou, Z., Song, J., Wang, C., Zuo, J., and Dong, X.** (2008). Plant immunity requires conformational changes [corrected] of NPR1 via S-nitrosylation and thioredoxins. *Science* **321**: 952–956.
- Taler, D., Galperin, M., Benjamin, I., Cohen, Y., and Kenigsbuch, D.** (2004). Plant eR genes that encode photorespiratory enzymes confer resistance against disease. *Plant Cell* **16**: 172–184.
- Torres, M.A., Dangl, J.L., and Jones, J.D.** (2002). *Arabidopsis* gp91phox homologues AtrbohD and AtrbohF are required for accumulation of reactive oxygen intermediates in the plant defense response. *Proc. Natl. Acad. Sci. USA* **99**: 517–522.
- van Damme, M., Zeilmaier, T., Elberse, J., Andel, A., de Sain-van der Velden, M., and van den Ackerveken, G.** (2009). Downy mildew resistance in *Arabidopsis* by mutation of HOMOSERINE KINASE. *Plant Cell* **21**: 2179–2189.
- Walters, D.R., and Bingham, I.J.** (2007). Influence of nutrition on disease development caused by fungal pathogens: Implications for plant disease control. *Ann. Appl. Biol.* **151**: 307–324.
- Wei, W., Plovianich-Jones, A., Deng, W.L., Jin, Q.L., Collmer, A., Huang, H.C., and He, S.Y.** (2000). The gene coding for the Hrp pilus structural protein is required for type III secretion of Hrp and Avr proteins in *Pseudomonas syringae* pv. tomato. *Proc. Natl. Acad. Sci. USA* **97**: 2247–2252.
- Wiermer, M., Feys, B.J., and Parker, J.E.** (2005). Plant immunity: The EDS1 regulatory node. *Curr. Opin. Plant Biol.* **8**: 383–389.
- Wildermuth, M.C., Dewdney, J., Wu, G., and Ausubel, F.M.** (2001). Isochorismate synthase is required to synthesize salicylic acid for plant defence. *Nature* **414**: 562–565.
- Wilkinson, J.Q., and Crawford, N.M.** (1993). Identification and characterization of a chlorate resistant mutant of *Arabidopsis* with mutations in both Nia1 and Nia2 nitrate reductase structural genes. *Mol. Gen. Genet.* **239**: 289–297.